

**Manuscript version: Author's Accepted Manuscript**

The version presented in WRAP is the author's accepted manuscript and may differ from the published version or Version of Record.

**Persistent WRAP URL:**

<http://wrap.warwick.ac.uk/164419>

**How to cite:**

Please refer to published version for the most recent bibliographic citation information.

**Copyright and reuse:**

The Warwick Research Archive Portal (WRAP) makes this work by researchers of the University of Warwick available open access under the following conditions.

Copyright © and all moral rights to the version of the paper presented here belong to the individual author(s) and/or other copyright owners. To the extent reasonable and practicable the material made available in WRAP has been checked for eligibility before being made available.

Copies of full items can be used for personal research or study, educational, or not-for-profit purposes without prior permission or charge. Provided that the authors, title and full bibliographic details are credited, a hyperlink and/or URL is given for the original metadata page and the content is not changed in any way.

**Publisher's statement:**

Please refer to the repository item page, publisher's statement section, for further information.

For more information, please contact the WRAP Team at: [wrap@warwick.ac.uk](mailto:wrap@warwick.ac.uk).

# 1 **Disordering effect of the ammonium cation accounts for anomalous enhancement of** 2 **heterogeneous ice nucleation**

3 Thomas F. Whale

4 Department of Chemistry, University of Warwick, Gibbet Hill Road, Coventry, CV4 7AL, UK

5 tom.whale@warwick.ac.uk

6 **ABSTRACT:** Heterogeneous nucleation of ice from supercooled water is the process responsible for  
7 triggering nearly all ice formation in the natural environment. Understanding of heterogeneous ice  
8 nucleation is particularly key for understanding the formation of ice in clouds, which impacts weather  
9 and climate. While many effective ice nucleators are known the mechanisms of their actions remain  
10 poorly understood. Some inorganic nucleators have been found to nucleate ice at warmer temperatures  
11 in dilute ammonium solution than in pure water. This is surprising, analogous to salty water melting at  
12 a warmer temperature than pure water. Here, the magnitude of this effect is rationalized as being due to  
13 thermodynamically favorable ammonium-induced disordering of the hydrogen bond network of ice  
14 critical clusters formed on inorganic ice nucleators. Theoretical calculations are shown to be consistent  
15 with new experimental measurements aimed at finding the maximum magnitude of the effect. The  
16 implication of this study is that the ice-nucleating sites and surfaces of many inorganic ice nucleators  
17 are either polar or charged and therefore tend to induce formation of hydrogen ordered ice clusters. This  
18 work corroborates various literature reports indicating that some inorganic ice nucleators are most  
19 effective when nominally neutral and implies a commonality in mechanism between a wide range of  
20 inorganic ice nucleators.

21

## 22 **Introduction**

23 The freezing of liquid water into solid ice is one of the most familiar and important phase transitions in  
24 both everyday experience and the natural world.<sup>1</sup> At atmospheric pressure solid ice  $I_h$  is the stable phase  
25 at temperatures between 0°C and about -210°C.<sup>2</sup> However, pure liquid water can supercool to  
26 temperatures below -40°C before freezing.<sup>3, 4</sup> This is because homogeneous nucleation, where ice  
27 clusters large enough to grow spontaneously form in truly pure supercooled water, is a strikingly slow  
28 process.<sup>5</sup> In the natural world the majority of ice nucleation is heterogeneous in nature, meaning a  
29 surface in contact with supercooled water catalyzes the formation of ice crystals.<sup>6</sup>

30 Heterogeneous nucleation of ice has been extensively studied due to its role in the atmosphere, where  
31 cloud glaciation temperatures are often controlled by the ice nucleating ability of the aerosol in cloud  
32 water droplets<sup>6, 7</sup> with consequent impacts on weather and climate.<sup>8, 9</sup> Ice nucleation is also of great  
33 relevance to cryobiology, the study of life at low temperatures, where the location and nature of ice  
34 formation can often determine how well biological material copes with low temperatures, both in  
35 environmental contexts<sup>10</sup> and medically-relevant cryopreservation procedures.<sup>11</sup> As such, a great deal  
36 is known about what substances do and don't nucleate ice well. Examples of effective ice nucleators  
37 include AgI,<sup>12, 13</sup> proteins from bacterial plant pathogens<sup>14</sup> and the mineral feldspar.<sup>15, 16</sup> However,  
38 understanding of the microscopic mechanism of heterogeneous ice nucleation is lacking, and is an area  
39 of substantial recent interest with a great deal of both experimental<sup>7</sup> and computational<sup>17</sup> work produced  
40 in the last few years.

41 Ice nucleation very often occurs from aqueous solution rather than from pure water. As such, the impact  
42 of aqueous solutes on the freezing temperature of water has been of interest since the 18<sup>th</sup> century<sup>18</sup> and  
43 the interaction of different nucleators with solutes has been intensively studied over the last 50 years.  
44 Improved understanding of the impact of solutes on heterogeneous nucleation has the potential to shed  
45 light on mechanism of heterogenous ice nucleation.

1 The ‘water activity criterion’ (WAC) developed by Koop et al.<sup>19</sup> accounts for colligative effects on ice  
2 nucleation, analogous to the familiar melting point depression observed in salty water. It states that  
3 there is a constant offset between the water activity of a solution at the ice-water equilibrium and the  
4 water activity at the freezing temperature. The offset for homogeneous ice nucleation  $\Delta a_{w,hom}$  was  
5 determined to be 0.311,<sup>19</sup> later updated to 0.314.<sup>20</sup> Subsequent work showed that solute induced changes  
6 in heterogeneous nucleation temperatures could also be described by the water activity criterion, with  
7 smaller values of  $\Delta a_w$ .<sup>21</sup> For instance, silica spheres used to induce freezing in picolitre scale emulsion  
8 droplets have been found to give  $\Delta a_{w,het}$  of 0.173. The smaller  $\Delta a_w$  indicates that the heterogeneous  
9 nucleation process takes place at warmer temperatures than homogeneous nucleation, due to a smaller  
10 free energy barrier to nucleation. The WAC can only account for depressions in nucleation temperature.

11 Recently, Kumar et al.<sup>22</sup> and Whale et al.<sup>23</sup> reported that ice nucleation induced by the mineral feldspar,  
12 known to be a highly effective nucleator,<sup>15</sup> was enhanced by low concentrations of various ammonium  
13 salts. The finding of enhancement is striking and means non-colligative effects must be in action. It is  
14 thought possible that ammonium salts in the atmosphere could make significant differences to the  
15 freezing temperatures of droplets in clouds<sup>22, 23</sup> and atmospheric condensation mode ice nucleating  
16 particle concentrations have been observed to increase in the presence of ammonium sulfate rich  
17 aerosol.<sup>24</sup>

18 Deviations from the WAC have also been observed for other mineral nucleators. To briefly summarize,  
19 feldspar, kaolinite, mica and gibbsite have all recently been found to nucleate ice at higher temperatures  
20 in dilute (0.01 M to about 0.1 M) ammonium solutions than in pure water.<sup>23, 25</sup> A similar result has been  
21 found for quartz,<sup>23</sup> although deactivation has also been observed.<sup>25, 26</sup> Other electrolytes have been found  
22 to impair ice nucleation by feldspars more than predicted by the WAC.<sup>27, 28</sup> Two studies observed that  
23 potassium salts can increase the temperature at which feldspars nucleate ice,<sup>27, 28</sup> although other studies  
24 have found the reverse, a reduction in nucleation temperature greater than that predicted by the WAC.<sup>23</sup>  
25 Amorphous silica and humic acid-type substances have been found to follow the WAC with all tested  
26 solutes.<sup>21, 23</sup>

27 In 1974 Reischel and Vali<sup>29</sup> reported freezing of 12  $\mu$ l droplets containing ‘kaolin’. Their data are  
28 largely compatible with findings of more recent studies, although it should be noted that the nucleator  
29 used may have contained minerals besides kaolinite, so may not be directly comparable to studies using  
30 the mineral kaolinite. They reported beyond-colligative suppressions of ice nucleation activity by NaI,  
31 NaCl, CsCl, K<sub>2</sub>SO<sub>4</sub> and KI. They also reported enhancements caused by 0.01 M and 0.1 M of NH<sub>4</sub>Cl,  
32 NH<sub>4</sub>Br, NH<sub>4</sub>I and 0.01 M (NH<sub>4</sub>)<sub>2</sub>SO<sub>4</sub>. 1 M concentrations of these salts started to inhibit ice nucleation  
33 activity. Reischel and Vali found a 12°C increase in freezing temperatures in 1 M LiI. A recent attempt  
34 to replicate this result with kaolinite did not see similar behavior.<sup>30</sup>

35 Several studies have looked at the impact of aqueous solutes on AgI, the archetypal and much studied  
36 ice nucleator whose activity was famously predicted by Bernard Vonnegut on the basis of its structural  
37 similarity to ice I<sub>h</sub>.<sup>12</sup> Macromolecular ‘anti-nucleators’ such as proteins, polymers and surfactants have  
38 been found to strongly inhibit the nucleating effectiveness of AgI. It has been reported that ice  
39 nucleation temperature of AgI dispersions can be reduced by up to 15.8°C by the presence of 1.0 mg/ml  
40 of polyvinyl alcohol.<sup>31</sup> Many other polymers and surfactants<sup>32</sup> reduce nucleation temperatures of AgI  
41 by around 10°C.<sup>33</sup> Zobrist and Koop<sup>21</sup> froze emulsions of picoliter scale solution droplets of various  
42 concentrations containing AgI particles. In the presence of (NH<sub>4</sub>)<sub>2</sub>SO<sub>4</sub> an anomalous increase in freezing  
43 temperatures was observed. This was attributed to changes in crystal habit caused by crystallization of  
44 AgI in the presence of NH<sub>4</sub><sup>+</sup>. The response to other salts including LiCl<sub>2</sub>, MgCl<sub>2</sub>, K<sub>2</sub>CO<sub>3</sub> and Ca(NO<sub>3</sub>)<sub>2</sub>  
45 followed the WAC.

46 Reischel and Vali<sup>29</sup> also froze droplets containing AgI particles together with varying concentrations of  
47 a range of electrolytes, including five ammonium salts. Complex and often large deactivations were  
48 observed with many non-ammonium salts. This was reasonably attributed to varying degrees of

1 solubilization of AgI in different salt solutions. Freezing temperatures were found to be raised in  
2 solutions of NH<sub>4</sub>I, NH<sub>4</sub>Br and NH<sub>4</sub>CNS although not NH<sub>4</sub>Cl.

3 Finally, recent work by Curland et al.<sup>34</sup> and Javitt et al.<sup>35</sup> found that ice nucleation on charged AgI and  
4 LiTaO<sub>3</sub> surfaces can be enhanced by nitrate, bicarbonate, guanidinium and biguanidinium<sup>34, 35</sup> ions.  
5 Guanidinium and biguanidinium were found to enhance negatively charged surfaces while nitrate and  
6 bicarbonate were found to enhance positively charged surfaces.

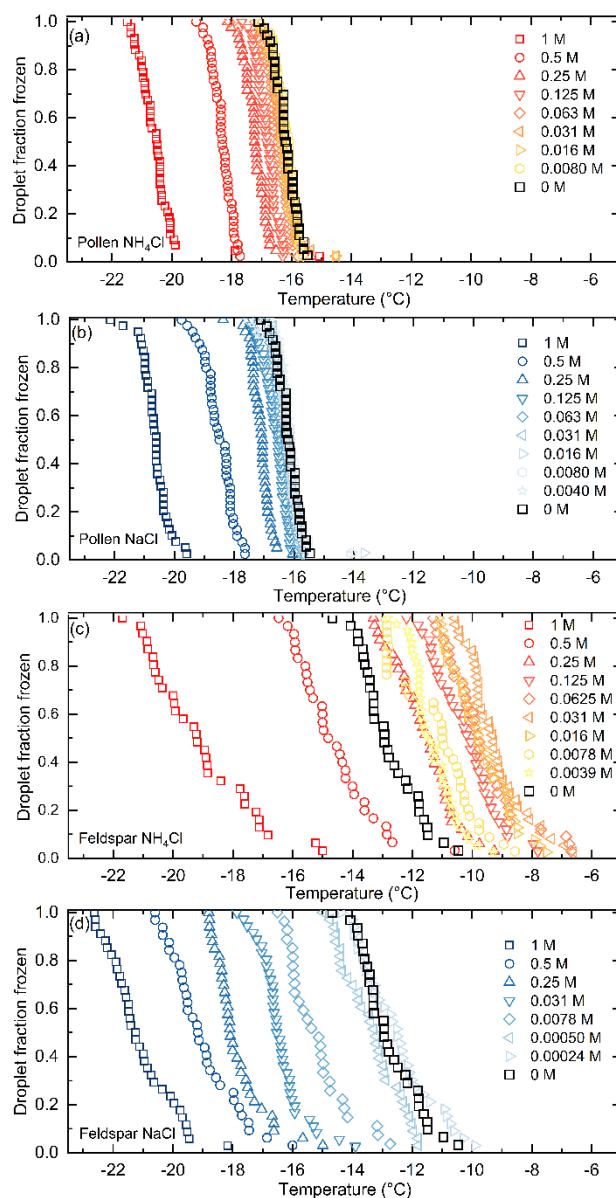
7 Overall, enhancement of heterogeneous nucleation on inorganic surfaces by solutes is almost unique to  
8 the NH<sub>4</sub><sup>+</sup> cation. Indeed, it has recently been proposed that enhancement in of ice nucleation on  
9 (NH<sub>4</sub>)<sub>2</sub>(SO<sub>4</sub>) solution might be used as an indicator for the presence of mineral dust ice nucleators in  
10 natural samples.<sup>36</sup> The only exceptions are enhancements to alkali feldspars caused by KCl and the  
11 contested enhancement to kaolin caused by LiI, as well as the recent findings of enhancement by various  
12 ions on charged surfaces. It is striking that the NH<sub>4</sub><sup>+</sup> induced enhancement been observed in AgI, various  
13 feldspars, kaolinite, muscovite mica, gibbsite and quartz. These materials all have quite different  
14 structures and presumably nucleate ice in different ways so the common response to the presence of  
15 NH<sub>4</sub><sup>+</sup> is, perhaps, surprising.

16 In this study I argue that polar and charged surfaces which tend to orient water molecules are likely  
17 responsible for the ice nucleation ability of many inorganic nucleators and that unexplained increases  
18 in heterogeneous nucleation temperatures caused by ammonium salts<sup>22, 23</sup> are likely due to the disruption  
19 of thermodynamically unfavorable hydrogen ordering of ice clusters induced by these water-orienting  
20 nucleating surfaces.

## 21 **Experimental measurements of enhancement and suppression of ice nucleation**

22 Fig. 1 shows heterogeneous nucleation data illustrating the unexplained deviations. To produce these  
23 measurements the freezing temperatures of 2 μl water droplets containing the known effective ice  
24 nucleators BCS 376 feldspar and pollen washing water (PWW) from *Betula pendula* the silver birch  
25 tree were measured. BCS376 was the alkali feldspar used in the first study<sup>15</sup> reporting feldspar's  
26 exceptional ice nucleating activity and has typical nucleation effectiveness for an alkali feldspar.<sup>37, 38</sup>  
27 PWW contains ice nucleating polysaccharides of unknown structure,<sup>39</sup> also thought to nucleate ice in  
28 the atmosphere.<sup>40, 41</sup>

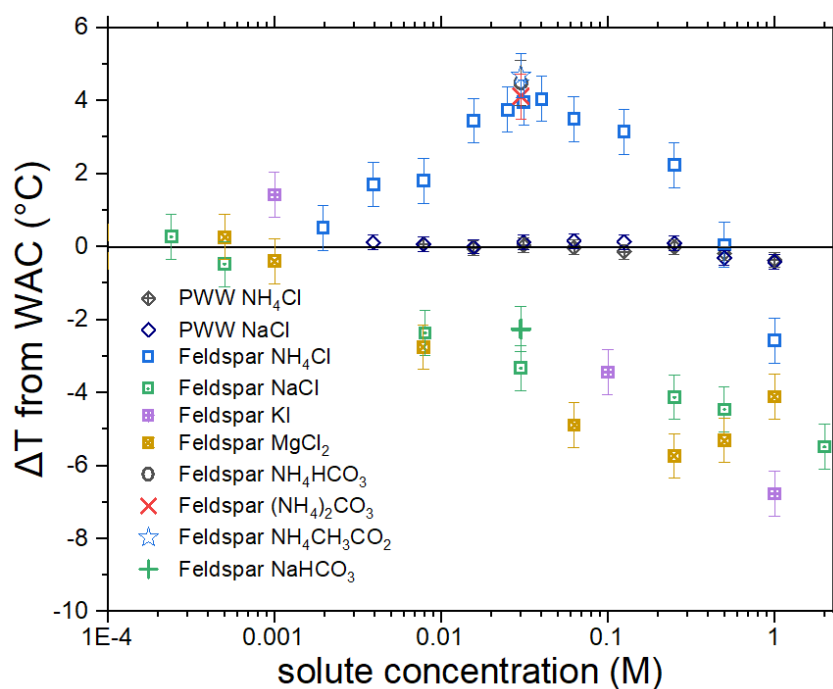
29 Experiments were conducted on an apparatus essentially similar to that described by Whale et al.<sup>42</sup>  
30 Approximately 40 one microliter droplets of either filtered PWW or a suspension containing 0.1 wt%  
31 of BCS376 feldspar were placed onto a silanised glass slide using an electronic pipette. One microliter  
32 droplets containing various concentrations of a range ammonium salts, NaCl, KI and MgCl<sub>2</sub> were then  
33 pipetted on top of the nucleator-containing droplets and the freezing experiment started immediately,  
34 minimizing the possibility of solute-induced aging of nucleators. The concentrations reported are the  
35 final concentrations of the resulting two microliter droplets. It can be seen that in NH<sub>4</sub>Cl solution  
36 freezing temperatures of feldspar droplets increases, while in NaCl droplets freezing temperatures are  
37 reduced to a greater extent than for PWW with similar salt concentrations.



1

2 Figure 1: Fraction frozen curves for 2  $\mu\text{l}$  droplets containing (a) Birch PWW in various concentrations  
 3 of  $\text{NH}_4\text{Cl}$  (b) Birch PWW in various concentrations of NaCl (c) 0.05 wt% BCS376 feldspar in various  
 4 concentrations of  $\text{NH}_4\text{Cl}$  and (d) 0.05 wt% BCS376 feldspar in various concentrations of NaCl.

5 In Fig. 2 the difference between observed average freezing temperatures for the nucleators and that  
 6 predicted by the WAC is shown. In the case of nucleation induced by PWW both  $\text{NH}_4\text{Cl}$  and NaCl  
 7 follow the water activity criterion at lower salt concentrations. There is a small negative deviation for  
 8 1 M and 0.5 M solutions.<sup>43</sup>



1

2 Figure 2: Deviation of nucleation temperature from that predicted by the WAC for the nucleators pollen  
 3 washing water and BCS376 feldspar in a variety of electrolytes.  $\Delta a_{w,het}$  was in both cases calculated  
 4 from the pure water measurement for both nucleators giving  $\Delta a_{w,het} = 0.117$  for BCS376 and  
 5  $\Delta a_{w,het} = 0.146$  for PWW. Confidence intervals were calculated using a Monte-Carlo simulation  
 6 described in section S2 of the supplementary information.

7 In contrast, Fig. 2 shows that heterogeneous ice nucleation induced by feldspar did not obey the WAC.  
 8 As expected the measurements for BCS376 in pure water indicated essentially identical activity to that  
 9 reported in Atkinson et al.<sup>15</sup> Figure S1 in the supplementary information shows a comparison of active  
 10 site density demonstrating this. At solute concentrations below  $5 \times 10^{-4}$  M, all measurements were  
 11 compatible with the WAC. At higher concentrations however, dissolved NaCl and MgCl<sub>2</sub> caused  
 12 steadily decreasing negative deviations from the expected colligative freezing temperature, indicating  
 13 an inhibition of heterogeneous nucleation. At 2 M this deviation is as much 6°C. Increasing  
 14 concentration of NH<sub>4</sub>Cl caused a steadily increasing positive deviation from the WAC up to 0.03 M,  
 15 where a nucleation temperature 4°C higher than expected was found. Measurements conducted using  
 16 0.025 M and 0.04M NH<sub>4</sub>Cl gave similar freezing temperatures, suggesting that the maximum  
 17 enhancement due to ammonium occurs in this sort of concentration range. Other ammonium salts tested  
 18 generated similar or slightly larger enhancements at 0.03M, up to 4.5°C, strongly suggesting that  
 19 concentration of NH<sub>4</sub><sup>+</sup> is the critical factor defining enhancement ice nucleation. At still higher  
 20 concentrations ice nucleation was anomalously suppressed by NH<sub>4</sub>Cl. MgCl<sub>2</sub> and KI generate broadly  
 21 similar degrees of non-colligative suppression to NaCl.

22 It seems obvious from these data to conclude that there are two competing effects; an enhancement  
 23 associated with the presence of NH<sub>4</sub><sup>+</sup> ions and a deactivation associated with all electrolytes, including  
 24 those containing NH<sub>4</sub><sup>+</sup> ion. The degree of suppression observed appears to depend to some extent on  
 25 the nature of the electrolyte. Experiments using KI revealed a small enhancement at  $1 \times 10^{-3}$  M as  
 26 reported by Yun et al.<sup>28</sup> for KNO<sub>3</sub>. These enhancements are much smaller than those reported by Perkins  
 27 et al.<sup>27</sup> in potassium salts. Higher concentrations of KI suppressed ice nucleation to a degree similar to  
 28 other non-ammonium salts.

29 These data are essentially compatible with those reported by Whale et al.<sup>23</sup> and Kumar et al.<sup>22</sup> In  
 30 particular, Figure 3 of Kumar et al.<sup>22</sup> reports very similar trends for ice nucleation by feldspar, both in

1 terms of enhancement by  $\text{NH}_4^+$  and suppression by other salts. In Kumar et al.<sup>22</sup> the maximum observed  
2 nucleation temperature was about  $-21^\circ\text{C}$  with a similar maximum enhancement of about  $4^\circ\text{C}$  observed.  
3 This occurred at the higher concentration of 0.103 M  $\text{NH}_4\text{Cl}$  solution, more concentrated than the  
4 concentration of maximum enhancement found here. The study of Whale et al.<sup>23</sup> found a smaller  
5 maximum increase in freezing temperature of around  $3^\circ\text{C}$  with identical freezing temperatures found in  
6 0.15 M and 0.015 M solutions suggesting that Whale et al.<sup>23</sup> missed the concentration of peak effect,  
7 concluding incorrectly that observed maximum increase in freezing temperature was due to a saturation  
8 effect.

9 Taking these new data with previous measurements we can conclude that a) the maximum degree of  
10 ammonium-induced enhancement of ice nucleation by feldspar is around  $4^\circ\text{C}$  or a little more,  
11 irrespective of the nucleation temperature of the feldspar in pure water b) all ammonium salts tested to  
12 date enhance ice nucleation by feldspar. The list of ammonium salts which have been tested now  
13 stretches to  $\text{NH}_4\text{Cl}$ ,  $\text{NH}_4\text{NO}_3$ ,  $(\text{NH}_4)_2\text{SO}_4$ ,  $\text{NH}_4\text{HSO}_4$ ,  $\text{NH}_3\text{OH}$ ,  $\text{NH}_4\text{HCO}_3$ ,  $(\text{NH}_4)_2\text{CO}_3$  and  $\text{NH}_4\text{CH}_3\text{CO}_2$   
14 c) the concentration  $\text{NH}_4^+$  is likely a key factor for enhancement of ice nucleation by feldspar and d)  
15 that ice nucleation by feldspar is suppressed by all salts, including ammonium salts, more than would  
16 be anticipated by the WAC. In the case of the ammonium salts this inhibition is overcome by the  
17 enhancing effect of ammonium at lower concentrations.

### 18 **The interaction of the $\text{NH}_4^+$ ion with ice**

19 As discussed in the introduction, enhancements to heterogeneous ice nucleation are observed across  
20 multiple inorganic nucleators, not just feldspar, when ammonium is present. What then is special about  
21 the ammonium cation and why does it enhance heterogeneous ice nucleation? Kumar et al.<sup>22</sup> argued  
22 that  $\text{NH}_3$  formed from excess  $\text{NH}_4^+$  adsorbs to the surface of feldspar, providing multiple hydrogen  
23 bonding opportunities directed into the water on the surface, enhancing ice nucleation effectiveness  
24 while Whale et al.<sup>23</sup> mentioned that ion adsorption, ion exchange with the substrate or an unknown  
25 aqueous phase effect could all potentially explain the observations. Molecular dynamics simulations  
26 aimed at resolving the question looking at both kaolinite<sup>30</sup> and feldspar<sup>43</sup> substrates found no  
27 enhancements to nucleation in the presence of  $\text{NH}_4^+$ . In total, there is no clear picture of why  $\text{NH}_4^+$  can  
28 enhance ice nucleation, or why other salts have non-colligative impacts on some nucleators.

29 It has long been known that  $\text{NH}_4^+$  has an unusual relationship with water and ice, being isostructural  
30 with the  $\text{H}_2\text{O}$  molecule.<sup>44</sup> Indeed,  $\text{NH}_4\text{F}$  is thought capable of forming co-crystals with water ice,<sup>45, 46</sup>  
31 meaning that individual  $\text{NH}_4^+$  cations can take the place of water molecules in the ice lattice. Other  
32 ammonium salts do not form co-crystals with ice, presumably because other anions do not fit into the  
33 ice lattice as  $\text{F}^-$  is apparently able to. The difference between  $\text{NH}_4^+$  and the water molecule is the number  
34 of hydrogen bonds donated and accepted.  $\text{H}_2\text{O}$  donates two bonds and accepts two bonds while  $\text{NH}_4^+$   
35 donates four bonds.

36 Recently, it has been found that  $\text{NH}_4\text{F}$  can act as a hydrogen disordering agent for ice.<sup>47-49</sup> The most  
37 profound impact of this is that water doped with small quantities of  $\text{NH}_4\text{F}$  cannot be frozen into ice II,  
38 the phase of ice stable at pressures above 0.2 GPa and below  $-40^\circ\text{C}$ . The structure of ice II relies on an  
39 ordered hydrogen bond network<sup>47</sup> and small amounts of  $\text{NH}_4\text{F}$  prevent its formation because the  
40 differences in number of bonds accepted and received when  $\text{NH}_4^+$  and  $\text{F}^-$  replace water molecules  
41 disrupts this order.

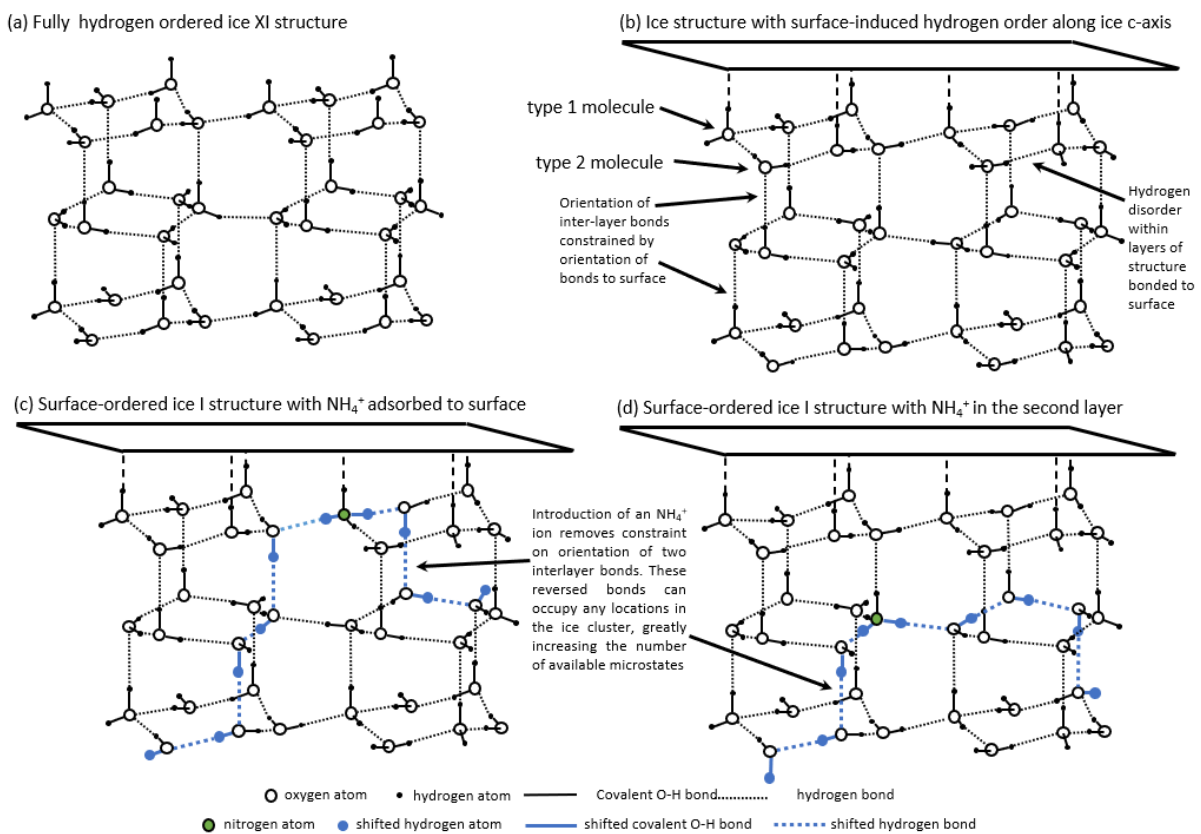
### 42 **Hydrogen ordering in ice $\text{I}_h$**

43 To understand the possible role of  $\text{NH}_4^+$  in heterogeneous ice nucleation we must consider the structure  
44 of ice which nucleates at atmospheric pressure. The third law of thermodynamics dictates that the ice  $\text{I}_h$   
45 structure, which is stable at atmospheric pressure and temperatures below  $0^\circ\text{C}$ , cannot be the ground  
46 state of the ice crystal because it is hydrogen disordered and its configurational entropy will therefore  
47 always be greater than zero. Linus Pauling calculated the residual entropy of a disordered ice I crystal

1 to be  $R \ln(3/2)$ .<sup>50</sup> Due to the slow kinetics of the phase transition to the ordered phase pure water ice  
 2 does not order on cooling to low temperatures.

3 It was eventually found that an ordered form of ice I, named ice XI, could be produced by doping the  
 4 ice with KOH.<sup>51</sup> At this point, it was determined that ice I<sub>h</sub> is the stable phase above about -201°C while  
 5 below that temperature ice XI is stable.<sup>51</sup> Structurally, they differ only in that ice XI, shown in Fig. 3(a),  
 6 is hydrogen ordered, meaning protons adopt the same locations throughout the crystal, while ice I<sub>h</sub> is  
 7 hydrogen disordered, meaning that the orientation of individual water molecules is random, although  
 8 constrained by the Bernal-Fowler ice rules, essentially meaning that only one hydrogen can sit between  
 9 each pair of oxygen atoms.<sup>52</sup>

10 It is possible to calculate the Gibbs free energy of ice XI as a function of temperature from the equation  
 11 of state of ice I<sub>h</sub><sup>53</sup> if it assumed that the enthalpy of the ice I-ice XI phase transition doesn't change with  
 12 temperature. In this way it can be shown that a hypothetical bulk ice XI would melt into liquid water at  
 13 about -29°C demonstrating substantially lower stability than ice I<sub>h</sub> at the temperatures of interest for  
 14 heterogeneous ice nucleation. Details of this calculation can be found in section S3 of the supplementary  
 15 information, where Fig. S3 shows the stabilities of ice I<sub>h</sub>, ice XI and supercooled water. Clearly, ordered,  
 16 low entropy ice is less stable than completely disordered, high-entropy ice at the temperatures (>-35°C  
 17 or so) generally of interest in the study of heterogeneous ice nucleation. While we should not expect ice  
 18 XI to nucleate at temperatures relevant for heterogeneous ice nucleation if a nucleator tends to induce  
 19 formation of partially hydrogen-ordered ice clusters we might expect that ice to be less  
 20 thermodynamically stable than completely disordered ice.



21  
 22 Figure 3: Schematic showing (a) the structure of fully hydrogen-ordered ice XI (b) a possible structure  
 23 of ice bound to a nucleating substrate which induces orientation of hydrogen atoms in the contact layer  
 24 towards itself (c) a possible structure of a similar ice crystal with one water molecule in the contact  
 25 layer replaced by an  $\text{NH}_4^+$  ion (d) a possible structure of a similar ice crystal with one water molecule  
 26 in the second bilayer replaced by an  $\text{NH}_4^+$  ion. In structures (c) and (d) two interlayer bonds can reverse



1 their orientation compared to structure (b). As there is no constraint on which bonds in a bilayer are  
2 reversed this offers the structure many more possible microstates, increasing its entropy.

### 3 **The role of $\text{NH}_4^+$ in heterogeneous ice nucleation**

4 Neville Fletcher suggested in 1959<sup>54</sup> that pristine basal faces of AgI and  $\text{PbI}_2$ , which are polar<sup>55</sup> would  
5 nucleate a partially hydrogen-ordered, low entropy form of ice. These nucleators are thought to be  
6 effective because their ionic surfaces can bond to water molecules and their structural similarity to ice  
7 means that interfacial water molecules adopt ice-like spatial locations, reducing the free energy barrier  
8 to nucleation, an epitaxial mechanism.

9 As discussed by Fletcher,<sup>54</sup> on such a surface, the energy of the interface with water will be minimized  
10 when the O-H dipole of a water molecule is parallel to the local electric field. The oxygen atoms of ice  
11  $\text{I}_h$  can be thought of as forming a layered structure, with each bilayer consisting of puckered 6-member  
12 rings of water molecules. In the bilayer next to the nucleating surface (hereafter the ‘contact bilayer’)  
13 there are two types of molecule. 1) Those with a bond to the surface and 2) those with a bond to the  
14 second layer of water molecules. Fig. 3 (b) shows a schematic of an ice  $\text{I}_h$  crystal adhered to a surface  
15 with water molecules next to the nucleating surface oriented in this manner. The orientation of the  
16 interlayer bonds of the first class of water molecules constrains the orientation of the second class of  
17 water molecules as both hydrogen atoms of these molecules must remain associated with in-layer bonds  
18 if there are to be enough in-layer hydrogens to satisfy the Bernal-Fowler ice rules. This means only lone  
19 pairs will be available to bond to the next ice bilayer. As such, orientational order will be transmitted  
20 through the entire ice-like structure. It is important to note that the structuring does not imply an ice XI  
21 structure of the type shown in Fig. 3 (a) as the in-layer bonds will still be disordered, as shown in Fig.  
22 3 (b). The same idea holds with the direction of all bonds reversed, in the case of a surface with positive  
23 charge or polarity. The entropy of polar ice I of the type shown in Fig. 3 (b) is thought to be close to  
24  $R \ln 20^{\frac{1}{24}}$ ,  $1.04 \text{ J K}^{-1} \text{ mol}^{-1}$  as calculated by Lipscomb<sup>56</sup> meaning it is substantially more ordered than  
25 Ice I, whose entropy is approximately  $R \ln \frac{3}{2}$ ,  $3.37 \text{ J K}^{-1} \text{ mol}^{-1}$ .

26 Fletcher<sup>54</sup> concluded that the polar basal face of AgI would mostly likely not nucleate ice well because  
27 it presents only either  $\text{Ag}^+$  or  $\text{I}^-$  ions to water and would therefore template formation of partially  
28 hydrogen ordered ice-like clusters, which would, due to their low entropy, have a low thermodynamic  
29 stability and therefore a low nucleation rate. Instead, he proposed that the prism faces of AgI most likely  
30 nucleate ice. These present alternating  $\text{Ag}^+$  and  $\text{I}^-$  ions and would be capable of nucleating a cluster with  
31 a fully disordered ice  $\text{I}_h$  structure, except in the first bilayer, which would be constrained to a single  
32 arrangement possessing hydrogen bonds of alternating direction.

33 The proposed role of  $\text{NH}_4^+$  in enhancing heterogeneous ice nucleation is shown schematically in Fig.  
34 3(c) and (d). In Fig. 3 the polarity of the nucleating surface requires a proton to sit on all bonds between  
35 the surface and the first ice bilayer. If an  $\text{NH}_4^+$  ion replaces a water molecule in the first ice bilayer it  
36 can both bond to the nucleator surface and donate three protons to the in-layer hydrogen bond network.  
37 In this way the obligation to donate a bond out-of-layer enforced on half the molecules in the structure  
38 is broken. Similarly, the obligation to bond in-layer forced on the other half of the molecules is broken.  
39 For each  $\text{NH}_4^+$  ion in the contact bilayer, two of the hydrogens bonds to the next layer can be reversed.  
40 This will offer an ice germ more possible microstates and increase its entropy. In effect, the critical  
41 cluster will be able to adopt a more disordered, stabler structure, while still forming an energetically  
42 favorable interface with the nucleator surface. This will increase the thermodynamic driving force to  
43 nucleation, raising nucleation temperature.

44 If an  $\text{NH}_4^+$  ion enters the second bilayer, as shown in Fig. 3(c) only this bilayer and those further from  
45 the surface are disordered; the entropy of bilayers closer to the nucleator surface will remain unchanged.  
46 If the polarity or charge of the nucleating surface is such that the lone pairs rather than the protons of

1 contacting water molecules are directed into the surface then  $\text{NH}_4^+$  induced disorder will propagate from  
2 higher bilayers towards the nucleating surfaces.

3 In the picture presented so far it has been assumed that surfaces induce orientation of all water molecules  
4 in the contact layer between critical cluster and nucleator. This need not be the case for  $\text{NH}_4^+$  to have  
5 an effect, as any partial induced orientation will necessarily result in a lower entropy, less stable  
6 structure which might be then disordered by the presence of  $\text{NH}_4^+$  although, clearly, the magnitude of  
7 the effect will be lessened. Further, the arguments put forward in this paper are based upon nucleation  
8 of ice  $I_h$  but apply also to nucleation of cubic ice  $I_c$  and stacking disordered ice  $I_{sd}$ , which are similarly  
9 layered structures. All water ices have very nearly the same configurational entropy due to hydrogen  
10 disorder<sup>57</sup> and it is not expected that the disordering mechanism should apply differently to different ice  
11 phases. A related point is that the arguments above apply equally well to ice  $I_h$  bound to a surface by  
12 the basal face and by the primary prism plane.

13 It is also worth discussing the nature of the phase nucleated by nucleators which tend to form polar ice  
14 clusters in the absence of  $\text{NH}_4^+$ . As mentioned, Fletcher<sup>54</sup> envisioned that in pure water the basal plan  
15 of AgI doesn't nucleate ice as the low-entropy phase templated is less stable than the disordered phase  
16 templated by the prism faces of AgI, despite the inferior lattice match of the prism faces. For the other  
17 nucleators enhanced by  $\text{NH}_4^+$ , feldspar, Gibbsite, kaolinite and mica, there is no obvious second crystal  
18 face which might reasonably be expected to nucleate ice. As such, it seems more likely that either a  
19 somewhat ordered crystal is nucleated from pure water, or that the energy cost of having some bonds  
20 in the contact layer oriented unfavorably contributes to the energy barrier to nucleation of a disordered  
21 critical cluster. In either case the change in entropy calculated next will have the same impact on  
22 nucleation rate and measured nucleation temperatures.

### 23 **The entropy of a heterogeneously nucleated critical cluster containing $\text{NH}_4^+$**

24 While a thorough assessment of the impact of the introduction  $\text{NH}_4^+$  on the entropy of an ice critical  
25 cluster will likely require molecular simulations an estimate of the magnitude of the change can be  
26 made. The entropy of a system is related to its multiplicity,  $\Omega$ , by Boltzmann's equation:

$$S = k \ln \Omega \quad (1)$$

27 Where  $k$  is the Boltzmann constant. As such, we must calculate the number of energetically equivalent  
28 microstates available to the ice critical cluster, with and without ammonium present. The assumption  
29 of energetic equivalence implicit in Eq. 1 will not be strictly correct for the smaller clusters discussed  
30 here, and calculation of the degree to which it is incorrect is a subject for simulation. As such,  
31 subsequent calculations neglect this complication. A second, related, assumption underpinning this  
32 work is that the presence of  $\text{NH}_4^+$  in the critical cluster doesn't change the energetics of the heterogenous  
33 ice nucleation process. Again, it is difficult to assess the impact of this assumption quantitatively  
34 however given only a small proportion of water molecules will be replaced by  $\text{NH}_4^+$  it seems likely the  
35 effect can be neglected. Finally, for most nucleating surfaces, the assumption of total order in the  
36 absence of  $\text{NH}_4^+$  is most likely incorrect. The implications of this are discussed later.

37 We shall first consider an ice critical cluster that is attached to the nucleator surface by its basal face  
38 and consists of a stack of bilayers each containing an equal number of water molecules. If the nucleating  
39 surface has a sufficient negative polarity or charge, as shown in Fig. 3, all protons in the contact and  
40 subsequent ice bilayers will point towards the nucleator surface, meaning  $\Omega$  for these protons equals 1.  
41 As mentioned, the entropy of the structure, taking into account this order, is approximately  $1.04 \text{ J K}^{-1}$   
42  $\text{mol}^{-1}$ .<sup>56</sup> Half of the water molecules in each bilayer have a bond to the next bilayer away from the  
43 nucleating surface. This number of bonds will be designated  $n_b$  meaning each bilayer contains  $2n_b$   
44 water molecules. As discussed, and shown in Fig. 3, addition of an  $\text{NH}_4^+$  ion to the bilayer in contact  
45 with a water-orienting nucleating surface will allow two of the interlayer bonds to the next layer to  
46 instead orient with a proton pointing away from the nucleating surface allowing us to calculate that, to

1 a first approximation,  $\Omega = \binom{n_b}{2}$  for that first bilayer, if it contains a single  $\text{NH}_4^+$  ion. This is because  
 2 we have  $n_b$  interlayer bonds of which any two can be oriented in the opposite direction to the rest of  
 3 the bonds. Because the same degree of disorder will be transmitted to each subsequent layer we can  
 4 estimate that the difference in total configurational entropy between an ice critical cluster containing a  
 5 single  $\text{NH}_4^+$  in the bilayer adjacent to the nucleating surface and one lacking the  $\text{NH}_4^+$  ion as

$$\Delta S_{\text{NH}_4^+, \text{cluster}} = k \ln \left( \frac{n_b!}{2!(n_b - 2)!} \right)^l \quad (2)$$

6 Where  $l$  is the number of ice bilayers in the critical cluster. The power  $l$  occurs because any of the  
 7 possible arrangements of the first bilayer can be paired with any possible arrangement of the second  
 8 bilayer, and vice versa, and so on for subsequent layers. For the broader case of  $n_{\text{NH}_4^+}$  ions in the first  
 9 bilayer of a critical cluster this can be generalised to

$$\Delta S_{\text{NH}_4^+, \text{cluster}} = lk \ln \left( \frac{n_b!}{(2n_{\text{NH}_4^+})!(n_b - 2n_{\text{NH}_4^+})!} \right). \quad (3)$$

10 We can see that according to Eq. 3  $\Delta S_{n_{\text{NH}_4^+}, \text{cluster}}$  depends on both the lateral extent and depth of the  
 11 cluster.

12 Equation 3 can be generalised to account for situations where bilayers are of unequal size, as would be  
 13 the case for any likely ice cluster geometry except a hexagonal prism, if it is assumed that all hydrogen  
 14 bonds reversed by the presence of  $\text{NH}_4^+$  bond to the next ice bilayer. If a reversed hydrogen bond forms  
 15 part of the interface of the critical cluster with liquid water, rather than a bond to next ice bilayer, it  
 16 would not be able to affect the orientation of bonds in that next ice bilayer. This would reduce the  
 17 number of configurations available to the cluster. The probability of this occurring will increase as the  
 18 difference in size between successive layers increases. Assuming that the effect is negligible (essentially  
 19 that there is a small difference in the extent of the top and bottom layers of the cluster) we can write

$$\Delta S_{\text{NH}_4^+, \text{cluster}} = lk \ln \left( \frac{\tilde{n}_b!}{(2n_{\text{NH}_4^+})!(\tilde{n}_b - 2n_{\text{NH}_4^+})!} \right) \quad (4)$$

20 where  $\tilde{n}_b$  is the mean number of water molecules in the  $l$  ice bilayers forming the critical cluster.  
 21 Clearly, these calculations neglect the reduction in entropy due to  $\text{NH}_4^+$  ions replacing water molecules,  
 22 meaning the replaced site will have fewer possible orientations, however it is reasonable to treat this  
 23 effect as minor as the number of orientations allowed to the replaced water molecule is already severely  
 24 constrained in the polar ice structure. Eqs. 2, 3 and 4 calculate the total entropy of an ice cluster. To  
 25 find the molar entropy we must divide by the number of water molecules in the cluster and multiply by  
 26 Avogadro's number. The number of molecules in the critical cluster is given by  $2n_b l$ . As such we can  
 27 write:

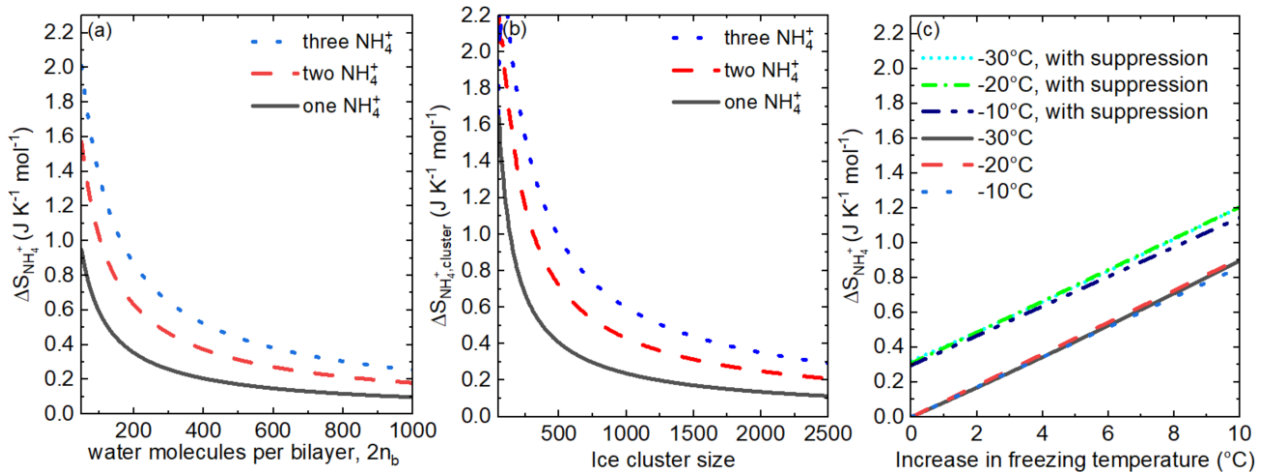
$$\Delta S_{\text{NH}_4^+} = \frac{R}{2\tilde{n}_b} \ln \left( \frac{\tilde{n}_b!}{(2n_{\text{NH}_4^+})!(\tilde{n}_b - 2n_{\text{NH}_4^+})!} \right) \quad (5)$$

1 Where  $\Delta S_{NH_4^+}$  is the molar difference in entropy between molecules in an ice cluster ordered by a  
 2 surface and a cluster with  $n_{NH_4^+}$   $NH_4^+$  ions in the contact bilayer, and  $R$  is the gas constant.

3 Fig. 4 (a) shows the variation in  $\Delta S_{n_{NH_4^+}}$  for one, two and three  $NH_4^+$  ions in the contact layer for various  
 4 values of  $\tilde{n}_b$  according to Eq. 5. It is clear that inclusion of more  $NH_4^+$  ions leads to a greater increase  
 5 in cluster entropy, and will therefore give a greater increase in nucleation temperature, consistent with  
 6 the experimental data in Fig. 2 where higher concentrations of  $NH_4^+$  lead to larger increases in freezing  
 7 temperature. It is also clear that differently shaped clusters will see different changes in entropy with  
 8 addition of ammonium ion as entropy difference per molecule is larger for clusters with a smaller lateral  
 9 extent.

10 According to classical nucleation theory (CNT) the size of heterogeneously nucleated ice critical  
 11 clusters varies relatively little with large changes in nucleation rate, falling in a range from a few  
 12 hundred to a few thousand water molecules at most.<sup>58</sup> As such, the range of water molecules per bilayer  
 13 shown in Fig. 4 (a) (50-1000) covers the likely range of cluster sizes and geometries for heterogeneous  
 14 ice nucleation in the temperature range of interest for this study. All things being equal, larger clusters  
 15 will tend to have more molecules per bilayer, hence smaller clusters will be impacted more the presence  
 16 of an  $NH_4^+$  ion, as might be expected.

17 Fig. 4 (b) shows the variation in  $\Delta S_{NH_4^+,cluster}$  with cluster size for a cluster three bilayers deep,  
 18 according to Eq. 4. Clearly, taller, narrower clusters containing an equivalent number of water  
 19 molecules would gain more entropy, shifting the curves up. The reverse would also be true.



20  
 21 Figure 4: (a) Difference in molar configurational entropy due to presence of one, two or three  $NH_4^+$  ions  
 22 in in the contact layer of a polar ice cluster as a function the number of water molecules in each ice  
 23 bilayer, according to Eq. 5. (b) Difference in molar configurational entropy as a function of cluster size  
 24 for a cluster containing three ice bilayers, according to Eq. 4. (c) Difference in molar configurational  
 25 entropy required to generate a given increase in heterogeneous freezing temperature according to Eq.  
 26 6. In all cases, a value of  $f_{het}$  which gave nucleation rate of  $10^{10}$  cm<sup>-2</sup> s<sup>-1</sup> at the indicated starting  
 27 temperatures was found. The entropy change is that required to give the same nucleation rate at the  
 28 warmer temperature. For the -10°C line  $f_{het} = 0.0259$ , for the -20°C line  $f_{het} = 0.117$  and for -30°C  
 29 line  $f_{het} = 0.281$ . To generate the ‘with suppression’ lines the experimental  $\Delta\mu_s$  due to 0.03M of NaCl,  
 30 82 J mol<sup>-1</sup> was subtracted, to account for the anomalous suppression to heterogeneous ice nucleation by  
 31 feldspar that appears to be common to all salts.

32 It will be apparent that this analysis contains a several simplifying assumptions. Due to the logarithmic  
 33 nature of the Boltzmann equation the assumption of complete transmission of disorder between layers  
 34 makes a fairly small difference to the entropy change due to  $NH_4^+$ . The section S7 of the supplementary

1 information details calculations of  $\Delta S_{NH_4^+,cluster}$  for ice clusters of 470 molecules of approximately  
2 spherical cap geometry showing that these more tapered shapes retain over 75% of the entropy change  
3 of a cluster with equal numbers of molecules in each bilayer, as calculated by Eq. 4. This cluster size  
4 was chosen as it is the size of the critical cluster for nucleated by feldspar in the CNT formulation used  
5 later in this paper. Larger clusters of similar geometry will retain more of the entropy change calculated  
6 by Eq. 4 while smaller cap-shaped clusters containing only 200 water molecules still retain more than  
7 70% of the entropy of equivalently sized cluster with equally sized layers.

8 All of the above assumes the nucleator tends to induce formation of ice clusters which are completely  
9 ordered orthogonal to the nucleating surface and completely disordered parallel to it, and so have the  
10 polar ice entropy calculated by Lipscomb.<sup>56</sup> It is possible to adapt the calculations above for cases where  
11 ice is partially disordered along its c-axis, meaning more than half but less than all of the inter-layer  
12 protons point towards the nucleator surface. This is discussed in section S8 of the supplementary  
13 information. As might be expected, larger numbers of  $NH_4^+$  ions are required to generate a given  
14  $\Delta S_{NH_4^+,cluster}$  when the fraction of bonds oriented by the surface is lower. As shown in Fig. S6,  
15 replacement of small numbers of water molecules with  $NH_4^+$  ions can still cause significant entropy  
16 changes to partially ordered clusters. For instance, the introduction of five  $NH_4^+$  molecules into the  
17 contact bilayer of a cluster containing 200 molecules in the contact bilayer ( $\tilde{n}_b = 100$ ) where 85% of  
18 bonds along the c-axis are oriented generates a  $\Delta S_{NH_4^+}$  of  $0.65 \text{ J K}^{-1} \text{ mol}^{-1}$ . Two  $NH_4^+$  ions are required  
19 to give a similar entropy change in a completely oriented cluster.

20 It is important to note that Eqs. 4 and 5 hold best for cases where there are relatively few  $NH_4^+$  ions in  
21 the critical cluster as they assume that the entropy of each bilayer is unaffected by the presence of the  
22 ions, which, as mentioned above, is a good approximation, rather than being strictly true. More complex  
23 calculations would need to be made for structures where  $NH_4^+$  ions are present in layers above the  
24 contact layer. Similarly, for the case where water lone pairs are oriented into the surface in the contact  
25 layer  $NH_4^+$  above the contact layer would induce disorder, and a different calculation would have to be  
26 made. In total, the complexity of the problem is difficult to approach thoroughly with calculations of  
27 the type conducted here and simulations will likely be required for a thorough analysis of all possible  
28 permutations of the mechanism. Nevertheless, it seems likely that the order of entropy change calculated  
29 and shown in Fig. 4 is reasonable.

### 30 **The impact of $NH_4^+$ ions on heterogeneous ice nucleation temperature**

31 Having estimated the potential increase in entropy of partially ordered ice clusters due to the presence  
32 of  $NH_4^+$  we now assess the increase in critical cluster stability needed to generate the experimentally  
33 observed changes in the temperature of ice nucleation induced by feldspar, assuming that feldspar tends  
34 to form polar ice-like clusters of the type shown in Fig. 3(b).

35 The underlying assumption behind the following approach is that all the anomalous differences between  
36 the observed freezing temperatures and those predicted by the WAC are due to solute-induced changes  
37 in the chemical potential of the ice cluster nucleated by a water-orienting surface caused by the presence  
38 of solutes. Fig. 2 clearly shows that in the case of ice nucleation by PWW dissolved NaCl and  $NH_4Cl$   
39 have exactly the same impact on nucleation temperatures. We can therefore confidently state that any  
40 impacts that NaCl and  $NH_4Cl$  have on diffusion activation free energy or the interfacial tension between  
41 ice and water are identical when the nucleator is PWW. It is possible that this is untrue when a nucleated  
42 ice cluster is polar, as is hypothesized to be the case for ice nucleation by feldspar. However, in the  
43 absence of suitable theory to account for any such effects, or even to predict whether they would help  
44 or hinder nucleation, we must assume that they are negligible for the purposes of these calculations.

45 According to classical nucleation theory (CNT), the stationary rate of heterogeneous nucleation,  
46 measured in nucleation events per surface area per unit time, can be found as<sup>59</sup>

$$J_{het}(T) = \frac{kT}{h} n_l \exp\left(\frac{-\Delta G_{diff}}{kT}\right) \exp\left(\frac{-f_{het}\Delta G_{crit}}{kT}\right) \quad (6)$$

1

2 Where  $k$  is the Boltzmann constant,  $T$  is absolute temperature,  $h$  is the Planck constant,  $n_l$  is the number  
 3 density of water molecules at the ice nucleus/water interface ( $\approx 10^{15} \text{ cm}^{-2}$ ),  $\Delta G_{crit}$  is the height of the  
 4 free energy barrier to forming a critical cluster of ice molecules and  $\Delta G_{diff}$  is the diffusion activation  
 5 free energy, calculated here using equation S5 derived by Koop and Murray.<sup>3</sup> It is assumed here that  
 6  $\Delta G_{diff}(T)$  is unaffected by the presence of dilute salts, as mentioned above, is an assumption but is  
 7 qualitatively supported by simulations.<sup>60</sup>  $f_{het}$  is a parameter taking values between zero and one. When  
 8  $f_{het} = 1$  the expression is equivalent to that for homogeneous nucleation<sup>3</sup> while for  $f_{het} = 0$  the barrier  
 9 to nucleation disappears. It is usual to relate  $f_{het}$  to a contact angle between a nucleating substrate and  
 10 a spherical cap shaped ice cluster in the manner described by Eq. S8. How close this description is to  
 11 the geometry of real ice critical clusters is not presently known.

12 The height of the free energy barrier to nucleation is given by

13

$$\Delta G_{crit}(T) = \frac{16\pi v_i^2 \sigma_{iw}^3}{3(\Delta\mu)^2} \quad (7)$$

14 where  $v_i$  is the molecular volume of a water molecule in ice,  $\sigma_{iw}$  is the ice-liquid interfacial energy and  
 15  $\Delta\mu$  is the driving force for ice nucleation, the difference in chemical potential between liquid water and  
 16 ice,  $\Delta\mu = \mu_{water} - \mu_{ice}$ .

17 It is generally accepted that homogeneous ice nucleation leads to the formation of stacking disordered  
 18 ice, ice  $I_{sd}$ , which has a mixture of hexagonal and cubic sequences.<sup>61-64</sup> Ice  $I_{sd}$  is metastable with respect  
 19 to normal ice  $I_h$  so its vapour pressure is higher. For heterogeneous ice nucleation it is not clear what  
 20 phase will nucleate as direct observation of the critical cluster is not presently possible.<sup>65</sup> Hence, while  
 21 the enthalpy difference between the ice  $I_{sd}$  and ice  $I_h$  can be estimated reasonably<sup>3</sup> here it is assumed  
 22 that the hexagonal phase forms. This allows use of an existing water activity dependent  
 23 parameterization for  $\sigma_{iw}$  in the presence of solutes, developed by Barahona<sup>66</sup>, which is given in equation  
 24 S6. The parameterisation predicts an increase in  $\sigma_{iw}$  with both increasing  $a_w$  and increasing  $T$  which is  
 25 qualitatively consistent with the result of molecular simulations of homogeneous ice nucleation.<sup>60, 67</sup>

26 In the current formulation of CNT, considering both colligative impacts on ice nucleation and the  
 27 anomalous effects reported here and elsewhere the driving force to nucleation,  $\Delta\mu$ , is given by

28

$$\Delta\mu(T, a_w) = kT \ln\left(a_w \left(\frac{p_w(T)}{p_i(T)}\right)\right) + \Delta\mu_s \quad (8)$$

29 where  $p_w(T)$  is the vapor pressures of supercooled water and  $p_i(T)$  is the vapour pressure of ice, both  
 30 parameterised by Murphy and Koop.<sup>68</sup>  $a_w$  is the water activity of the solution, calculated using the AIM  
 31 model<sup>69</sup> and assumed to change little with temperature.<sup>20</sup>  $\Delta\mu_s$  is the anomalous change in chemical  
 32 potential due to the presence of a solute.

1 We wish to compare  $J_{het}(T)$  calculated using Eq. 6 to experimental results. Ice nucleation by feldspar  
 2 is known to be site-specific, meaning that small patches of the surface are responsible for experimentally  
 3 observed ice nucleation activity.<sup>70, 71</sup> For the PWW we do not know the quantity or surface area of the  
 4 ice-active substance present in each droplet. As such, we cannot straightforwardly work out  $J_{het}$  for  
 5 feldspar or PWW for the data reported in Fig. 1 and Fig. 2. Happily, we are interested in changes in  
 6 nucleation temperature between experiments that detect essentially identical nucleation rates so we can  
 7 simply choose an ‘observable’  $J_{het}$  then calculate the change in driving force required to generate the  
 8 experimentally observed change in average nucleation temperature.

9 Here, observable  $J_{het}$  for feldspar is taken to be  $10^{10} \text{ cm}^{-2} \text{ s}^{-1}$ . The reasons for this are discussed in the  
 10 SI in some depth. Briefly, it is possible to estimate the number of ice nucleation active sites per feldspar  
 11 surface area per droplet at the temperatures used in this study due to the work of Holden et al.<sup>70</sup> and  
 12 possible to estimate the size of an ice nucleation active site using CNT, if the critical cluster is assumed  
 13 to be spherical cap. Combining these two things a likely order of nucleating surface area per droplet  
 14 can be determined. It is important to note that subsequent arguments do not depend strongly on the  
 15 specific value of  $J_{het}$  used. The value of  $\Delta\mu_s$  determined varies by less than 10% between a chosen rate  
 16 of  $1 \text{ cm}^{-2} \text{ s}^{-1}$  and  $10^{20} \text{ cm}^{-2} \text{ s}^{-1}$ .

17 In this formulation of CNT the change in nucleation rate due to the WAC can be calculated using  
 18 equations 6, 7, 8, S5 (to determine  $\Delta G_{diff}(T)$ ) and S6 (to determine  $\sigma_{iw}(T, a_w)$ ) if  $\Delta\mu_s$  is taken to be  
 19 zero. Fig. S4 shows that for ice nucleation induced by PWW in NaCl and  $\text{NH}_4\text{Cl}$  experimentally  
 20 measured reductions in nucleation temperature shown in Fig. 2 can be accounted for using a single  
 21 value of  $f_{het}$ . This demonstrates that CNT, appropriately adapted to account for changes in  $a_w$ , can  
 22 account for variation in ice nucleation temperature in PWW in the presence of solutes.

23 Clearly, the anomalous changes in nucleation temperature observed for feldspar can’t be accounted for  
 24 in this way so we must consider  $\Delta\mu_s$ . We can solve Eq. 6 to find the value of  $f_{het}$  required to give a  
 25 nucleation rate of  $J_{het} = 10^{10} \text{ cm}^{-2} \text{ s}^{-1}$  at  $-12.8^\circ\text{C}$ , the average nucleation temperature observed for the  
 26 feldspar suspension used in pure water. In this way  $f_{het} = 0.0438$  was determined as characteristic for  
 27 the feldspar in the experimental system used. Note that this value is entirely specific to the system, and  
 28 the somewhat arbitrary choice of  $J_{het}$ , and should not be taken as being characteristic for feldspar as an  
 29 ice nucleator generally. We can then find the  $\Delta\mu_s$  required to shift nucleation temperature from  $-12.8^\circ\text{C}$ ,  
 30 as observed in pure water, to  $-16.4^\circ\text{C}$ , as observed in 0.03M NaCl by using Eq. 6 and Eq. 8 at the lower  
 31 temperature and  $a_w$ . In this way  $\Delta\mu_s$  was found to be  $78.0 \text{ J mol}^{-1}$ . We can then solve Eq. 6 again to  
 32 find the  $\Delta\mu_s$  required to induce nucleation at  $-9.2^\circ\text{C}$ , the average nucleation temperature for feldspar in  
 33 0.03M  $\text{NH}_4\text{Cl}$ , giving  $-86.3 \text{ J mol}^{-1}$ . These values take into account the colligative effects predicted by  
 34 the WAC, although these are so small as to be effectively negligible, due to the low solute concentration  
 35 used. It can be seen in Fig. 1 (a) and (b) that 0.03M  $\text{NH}_4\text{Cl}$  and NaCl cause no measurable change in  
 36 freezing temperatures of droplets containing PWW.

37 To facilitate estimation of the amount of stabilisation of the critical ice cluster formed by feldspar that  
 38 would need to be provided by its  $\text{NH}_4^+$  induced disordering to account for the observed changes in  
 39 nucleation temperature we shall assume  $\Delta\mu_s$  is composed of the enhancing and inhibitory influence due  
 40 to solutes giving

$$\Delta\mu_s = \Delta\mu_{electrolyte} - \Delta\mu_{\text{NH}_4^+, \text{experiment}} \quad (9)$$

41 where  $\Delta\mu_{electrolyte}$  is the anomalous reduction in driving force due to the presence of all salts,  
 42 hypothesised later to be related to increased effective solute concentration in the vicinity of a charged  
 43 or polar nucleating surface, and  $\Delta\mu_{\text{NH}_4^+, \text{experiment}}$  is the increase in driving force due to favourable  
 44 disordering of the ice germ allowed by the presence of  $\text{NH}_4^+$ . Using Eq. 9 implies that all anomalous

1 changes in nucleation rate, both enhancement and suppression, are due to change in the stability of ice  
2 rather than changes in the interfacial tension, changes in  $f_{het}$  caused by the solutes, or changes in the  
3 activation energy, which may not be physically accurate. However, the magnitude of  $\Delta\mu_{NH_4^+, experiment}$   
4 determined would not be changed if the magnitude of the anomalous suppression were accounted for  
5 differently.

6 As there is no  $NH_4^+$  present in the 0.03M NaCl experiment we can use Eq. 9 to calculate that  
7  $\Delta\mu_{electrolyte}$  is 78.0 J mol<sup>-1</sup> for 0.03M NaCl. Using Eq. 9 and assuming that  $\Delta\mu_{electrolyte}$  is similar for  
8 NaCl and  $NH_4Cl$  at similar concentration we can calculate that  $\Delta\mu_{NH_4^+}$  is 164.3 J mol<sup>-1</sup>. If it is assumed  
9 that this change is entirely entropic in origin, we can divide this by the absolute nucleation temperature  
10 to find that the configurational entropy difference between the structure nucleated in the absence of  
11  $NH_4^+$  and that nucleated in the presence of  $NH_4^+$ ,  $\Delta S_{NH_4^+, experiment}$ , is 0.62 J K<sup>-1</sup> mol<sup>-1</sup>.

12 As discussed, the entropy change of polar ice clusters expected due to addition of ammonium ions  
13 depends on the shape and size of the cluster. The geometry of heterogeneously nucleated ice clusters is  
14 discussed in section S6 of the supplementary information. Assuming spherical cap critical cluster  
15 geometry, a nucleation rate of 10<sup>10</sup> cm<sup>-2</sup> s<sup>-1</sup> requires  $f_{het} = 0.0438$  which can be shown to correspond to  
16 spherical cap shaped critical cluster containing 470 water molecules, using Eq. S7. This spherical cap  
17 is the height of ice 3 bilayers, as shown in Table S1. If we look at Fig. 4 (b) we can see that two  $NH_4^+$   
18 ions in the contact bilayer of such a cluster would increase its entropy by 0.75 J K<sup>-1</sup> mol<sup>-1</sup>. As mentioned,  
19  $\Delta S_{NH_4^+}$  will only be around 75% of that of a cluster with evenly sized layers as calculated by Eq. 5,  
20 giving a value of 0.57 J K<sup>-1</sup> mol<sup>-1</sup>, as detailed in Table S2, close to the value determined for  
21  $\Delta S_{NH_4^+, experiment}$ .

22 In a 0.03M solution of  $NH_4Cl$  there will be only 1  $NH_4^+$  ion per approximately 1850 water molecules  
23 suggesting that on average the critical cluster may contain less than one  $NH_4^+$  ion. However, it is likely  
24 that there will be a higher than bulk concentration of ions near a charged or polar nucleating surface  
25 capable of orienting water molecules than in bulk solution. As such having two or more  $NH_4^+$  ions in a  
26 critical cluster does not seem implausible.

27 More generally, it is possible to calculate the  $\Delta S_{NH_4^+}$  required to generate a given increase in nucleation  
28 temperature using the method described above. Fig. 4 (c) shows the outcome of these calculations for  
29 heterogeneous nucleation of ice, starting from various temperatures, and both accounting for the general  
30 ice nucleation suppressing effect of ions demonstrated in Fig. 2 and not accounting for it. It can be seen  
31 that the required entropy differences are in the range accounted for by the proposed disordering  
32 mechanism.

33 While these calculations make various assumptions of uncertain veracity it seems reasonable to  
34 conclude that the amount of stability provided to an otherwise-polar ice cluster by the presence of  $NH_4^+$   
35 ions is of the order to drive the increases in nucleation temperature observed experimentally. Depending  
36 on interfacial concentration of  $NH_4^+$ , the geometry of the critical cluster and the degree of order imposed  
37 by the nucleator quite a large range of enhancements are conceivable, as shown in Fig. 4. Experimental  
38 results presented here suggest that the maximum increase in nucleation temperature on feldspar due to  
39 the presence of  $NH_4^+$  ions is around 4.5°C. The proposed disordering mechanism is easily capable of  
40 providing the enough stability to a critical cluster to account for this change. An upper limit to the  
41 entropy change due to disordering of is the difference in entropy between polar ice and completely  
42 disordered ice, 2.33 J K<sup>-1</sup> mol<sup>-1</sup>. In reality the upper limit is likely somewhat lower as incorporation of  
43 larger number of  $NH_4^+$  ions into an ice cluster will at some point become energetically unfavourable.  
44 However, Fig. 4 shows that even the 9°C enhancement observed by Worthy et al.<sup>36</sup> for kaolinite requires  
45 only around 1.1 J K<sup>-1</sup> mol<sup>-1</sup> of disordering which can be accounted for by including only 3  $NH_4^+$  ions in  
46 a cluster of the order of size anticipated by CNT.



## 1 **The role of anions**

2 The experimental data presented in Fig. 2 and elsewhere<sup>22, 23</sup> suggests that the ammonium effect on ice  
3 nucleation caused by feldspar is anion-independent. The data of Reischel and Vali<sup>29</sup> suggests that the  
4 identity of the anion does matter for ice nucleation by AgI, however this is likely influenced by the  
5 variable solubility of AgI in the presence of different anions.

6 It is well known that freezing ice excludes most solute molecules, with progressive concentration of  
7 liquid surrounding growing ice occurring until the eutectic composition is reached. It seems likely that  
8 a critical ice germ would be free of solute molecules as they would presumably substantially raise the  
9 free energy of any ice-like cluster they were part of, favoring a return to a liquid-like arrangement.  
10 Indeed, the so-called ‘unmixing’ energy required to create a solute free ice germ has been suggested as  
11 the origin of the WAC.<sup>66, 72</sup> It is known that NH<sub>4</sub>F incorporates readily into ice<sup>45, 46</sup> and also that NH<sub>4</sub>Cl  
12 is around five times more soluble in ice than HCl, LiCl, NaCl, KCl, RbCl and CsCl.<sup>73</sup> It therefore seems  
13 quite possible that NH<sub>4</sub><sup>+</sup> can incorporate into the ice hydrogen bond network without significantly  
14 raising the structure’s free energy, in contrast to other ions. Given the ice germ likely consists of at most  
15 1000 molecules or so while a 0.03M solution contains, as mentioned, only 1 solute molecule for every  
16 1850 water molecules it seems reasonable to suggest that clusters containing only NH<sub>4</sub><sup>+</sup> and no counter  
17 ions could come into existence.

## 18 **The origin of anomalous suppression of ice nucleation by electrolytes**

19 The necessary proximity of ions to polar surfaces raises a second intriguing possibility; that the non-  
20 colligative inhibiting impact of most non-ammonium salts on ice nucleation by feldspar and AgI is due  
21 to the energy cost of incorporating the charge balancing adsorbed ions, the effective concentration of  
22 which would be increased by the polar surface, into the ice germ anchored to the ice surface. It could  
23 also be that the energy penalty of moving these ions away from the surface accounts for the anomalously  
24 reduced nucleation rates observed. One or both of these effects may well be the origin of the  
25  $\Delta\mu_{electrolyte}$  term introduced above.

26 Interplay between the enhancing and inhibitory effects on ice nucleation by feldspar must lead to the  
27 observed peak in ice nucleation temperatures at an NH<sub>4</sub><sup>+</sup> concentration of 0.03M. The experimental data  
28 suggests that the disordering mechanism can work low NH<sub>4</sub><sup>+</sup> concentrations, which is consistent with  
29 the framework presented here, and that higher ion concentrations are required before the suppressing  
30 effect overwhelms it. Calculation or measurement of ion concentrations near charged and polar surfaces  
31 is complex and remains challenging however emerging methods may allow calculations of the likely  
32 impact of such effects to be made soon,<sup>74, 75</sup> facilitating comparison with experimental data of the type  
33 produced here.

34 It is perhaps surprising that Zobrist et al.<sup>21</sup> did not see anomalous suppression of ice nucleation activity  
35 of AgI by non-ammonium salts. One explanation of this is that, according to Fletcher<sup>54</sup> ice nucleates on  
36 the non-polar prism faces of AgI. These would not attract an excess of ions and may not be impeded by  
37 the suggested mechanism. However, in the presence of NH<sub>4</sub><sup>+</sup> ions the entropy penalty of ice clusters on  
38 the basal face of AgI, which has a better lattice match to ice than the prism face, may be relieved  
39 allowing it to take over as the ice-nucleating face.

## 40 **Suppression of ice nucleation by macromolecules**

41 The anomalous suppression of ice nucleation by AgI by various organics macromolecules<sup>33</sup> is  
42 potentially consistent with the idea that the nucleating surface of AgI is polar, contrary to the analysis  
43 of Fletcher<sup>54</sup> as such molecules would be likely to bond to polar surfaces. It seems possible that feldspar,  
44 mica, kaolinite and Gibbsite will also experience anomalous suppression to their ice nucleation  
45 temperatures in the presence of many organic macromolecules. This may plausibly have implications

1 for ice nucleation in mixed-phase clouds droplets which often contain organic compounds and mineral  
2 dusts.

### 3 **The nature of ice-nucleating surfaces**

4 An important implication of the proposed mechanism is that, if it is correct, ice nucleators whose  
5 activities are enhanced in  $\text{NH}_4^+$  solution must induce nucleation through the action of polar or charged  
6 surfaces capable of orientating water. The nucleators known to respond anomalously to  $\text{NH}_4^+$  are AgI,  
7 mica, Gibbsite and kaolinite. AgI is one of the examples given by Fletcher<sup>54</sup> and its (100) face is known  
8 to be polar.<sup>55</sup> The basal plane of kaolinite, which is thought to be responsible for kaolinite's ice  
9 nucleation activity,<sup>76</sup> is also polar.<sup>77</sup> The (001) surface of gibbsite is charged at pH below about 7<sup>78</sup> as  
10 it would be in  $\text{NH}_4^+$  solutions of the type used for ice nucleation experiments.<sup>25</sup> Mica surfaces are  
11 charged at various pHs so are likely also be capable of imposing order on forming ice clusters as  
12 discussed later. The (100) face of microcline feldspar, thought to responsible for its activity<sup>16, 79</sup> is, by  
13 inspection, also likely to be polar.

14 It is very important to note that polar surfaces are intrinsically unstable.<sup>80</sup> Polarity compensation can  
15 occur either in a manner intrinsic to the crystal (e.g. surface reconstruction), or by the adsorption of  
16 ions. The latter scenario was investigated by Sayer and Cox,<sup>55</sup> who found that ions from solution  
17 stabilized unreconstructed polar surfaces of AgI on timescales relevant to ice nucleation. Sayer and  
18 Cox<sup>55</sup> also provided tentative evidence for ion specificity of the heterogeneous nucleation rate, which  
19 would be inconsistent with the WAC. The common observation of site-specificity of ice nucleation<sup>81</sup>  
20 may be due, at least in part, to the rarity and instability of polar or charged patches of lattice-matching  
21 surface on ice nucleators.

### 22 **Ice nucleation by feldspar**

23 Considering the case of ice nucleation by feldspar, the calculations performed here to establish the  
24 amount of entropy needed to account for the observed maximum enhancement in nucleation  
25 temperature were also applied to the data of Kumar et al.<sup>22</sup> which were conducted with much smaller  
26 amounts of feldspar in each droplet. This lead to a freezing temperature in pure water of around  $-26^\circ\text{C}$   
27 against  $-12.8^\circ\text{C}$  in the present study. They observed a maximum increase in nucleation temperature of  
28  $4.5^\circ\text{C}$ . By using the suppression observed for a  $\text{Na}_2\text{SO}_4$  with equivalent water activity to calculate  
29  $\Delta\mu_{\text{electrolyte}}$  a maximum  $\Delta\mu_{\text{NH}_4^+}$  of  $156.6 \text{ J mol}^{-1}$  was determined, equivalent to  $\Delta S_{\text{NH}_4^+, \text{experiment}}$  of  
30  $0.61 \text{ J K}^{-1} \text{ mol}^{-1}$ , very similar to that determined for the experiments presented here, and similarly  
31 consistent with the proposed disordering mechanism.

32 Whale et al.<sup>82</sup> and Kiselev et al.<sup>83</sup> have shown that microtextural features on feldspars are responsible  
33 for their ice nucleation activities and argued that the exposure of different amounts of the (100) face  
34 hypothesised to be responsible for the nucleation activity of feldspars<sup>16</sup> may account for the different  
35 activities of different feldspars. That roughly the same magnitude of enhancement is observed  
36 irrespective of the ice-nucleating effectiveness and quantity of the feldspar used strongly suggests that  
37 a similar ice nucleation mechanism is in action in both active and inactive feldspars ice nucleation sites.  
38 The disordering mechanism predicts quite small changes in  $\Delta S_{\text{NH}_4^+, \text{cluster}}$  as cluster size varies, as can  
39 be seen in Fig. S4(b). As such, different sized patches of (100) face would experience broadly similar  
40 enhancements in ice nucleation temperature via the disordering mechanism as be seen in so the idea  
41 that more ice nucleation-active feldspars possess larger patches of exposed (100) face seems  
42 qualitatively consistent.

### 43 **Ice nucleation by mica and other water-orienting surfaces**

44 Recently, two studies<sup>84, 85</sup> have found that the ice nucleation ability of natural potassium mica can be  
45 substantially increased by ion exchange with  $\text{H}^+$ ,  $\text{Na}^+$ ,  $\text{Rb}^+$ ,  $\text{Cs}^+$ ,  $\text{Sr}^{2+}$ ,<sup>85</sup>  $\text{Ca}^{2+}$ ,  $\text{Mg}^{2+}$  and  $\text{Al}^{3+}$ .<sup>84</sup> Jin et al.<sup>85</sup>  
46 used sum frequency generation spectroscopy (SFG) to show that the mica surfaces which nucleated ice

1 well oriented water to a lesser extent than those which nucleated ice poorly. This agrees entirely with  
2 the mechanism proposed in the present study. Similarly, Abdelmonem et al.<sup>86</sup> found that a sapphire  
3 surface nucleated ice best in lower pH conditions and used SFG to show that these conditions led to  
4 disordered interfacial water. Again, this agrees with the proposed ammonium-disordering mechanism.  
5 We might predict that introduction of  $\text{NH}_4^+$  would enhance ice nucleation by sapphire at higher pHs  
6 where interfacial water is ordered but not in pH conditions where interfacial water is disordered.  
7 Looking forward, SFG might be used to generate a greater insight into the nature of ammonium-induced  
8 disordering of ice clusters.

## 9 **Enhancement of ice nucleation by guanidinium and biguanidinium**

10 As briefly mentioned in the introduction, it has recently been found that ice nucleation on the positively  
11 charged face of  $\text{LiTaO}_3$  and  $\text{AgI}$  can be enhanced by addition of  $\text{HCO}_3^-$  and  $\text{NO}_3^-$  while ice nucleation  
12 on the negatively charged face of  $\text{LiTaO}_3$  can be enhanced by the guanidinium and biguanidinium  
13 ions.<sup>34, 35</sup> These papers suggest that the ions tend to encourage the formation of hexagonal ice clusters,  
14 thereby favouring ice nucleation. Work by the same authors found that ice nucleation on  $\text{LiTaO}_3$  and  
15 pyroelectric amino acids varied with pH also.<sup>87</sup> It is worth noting that guanidinium and biguanidinium  
16 bear a strong structural resemblance to the ammonium ion. Guanidinium consists of three amino group  
17 bonded to a central carbon atom for instance. These ions would, if dissolved in an ice structure, offer  
18 only hydrogens and no lone pairs to the hydrogen bond network and might therefore be capable of  
19 inducing hydrogen disorder in ice. Given that  $\text{HCO}_3^-$  and  $\text{NO}_3^-$  enhance ice nucleation on the positively  
20 charged surfaces it seems possible that these ions, which would donate lone pairs into a hydrogen-bond  
21 network, also have a disordering effect when ice is nucleated by a positively charged surface.

22 Future work should certainly be directed at establishing whether guanidinium and biguanidinium  
23 enhance the same range of nucleators as the ammonium ion and at establishing whether the two  
24 proposed mechanisms of ice nucleation enhancement, entropically favourable hydrogen-disordering  
25 proposed here and enhanced cluster formation as proposed by and Curland et al<sup>34</sup> Javitt et al<sup>35</sup> are  
26 compatible and whether they might interact.

## 27 **Atmospheric implications**

28 As well as being of substantial fundamental interest, the mechanism of ice nucleation enhancement  
29 proposed here has important consequences for understanding of heterogeneous ice nucleation in the  
30 environment. Kumar et al.<sup>22</sup> and Whale et al.<sup>23</sup> both argued that enhancement of the ice nucleation  
31 ability of feldspar could influence cloud properties. If the ice-nucleating sites of most mineral dusts are  
32 indeed charged or polar this could also have important implications for their interactions with the  
33 soluble organic molecules known to be present in many cloud droplets,<sup>88, 89</sup> particularly organic acids.  
34 In general, prediction of the interaction of the interaction of atmospheric ice nucleating particles with  
35 solutes, and their aging pathways, may be facilitated by this finding.

## 36 **Conclusions**

37 To summarize, it is proposed here that the anomalous enhancement of heterogeneous ice nucleation in  
38  $\text{NH}_4^+$  containing solutions is due to the relief of unfavorable configurational entropy caused by  
39 nucleator-surface-induced ordering of the hydrogen bond networks of ice clusters. The magnitude of  
40 the effect is estimated on the basis of statistical mechanical arguments and demonstrated to be capable  
41 of accounting for experimentally observed changes in nucleation temperature, in both the present study  
42 and previous studies.

43 If this picture is correct those nucleators which do not respond anomalously to  $\text{NH}_4^+$  ions, which  
44 includes all biological nucleators that have been tested, amorphous silica and alcohol monolayers, must  
45 tend to induce formation of hydrogen-disordered ice clusters while nucleators that are anomalously  
46 enhanced by  $\text{NH}_4^+$ , namely feldspar, mica, kaolinite, Gibbsite and  $\text{AgI}$ , possess either polar or charged

1 sites or surfaces responsible for their observed ice nucleation activity. This work is consistent with  
2 previous findings of enhancement of ice nucleation in conditions of greater interfacial disorder of water,  
3 and ties together the ice nucleation mechanisms of a wide range of inorganic ice nucleators. This has  
4 important implications for ongoing work, both experimental and computational, aimed at understanding  
5 the mechanism of heterogenous ice nucleation, with further implications for understanding of the role  
6 of ice nucleation in the environment.

## 7 **Experimental Methods**

8 The data shown in Fig. 1 and Fig.2 were produced using a droplet freezing assay essentially similar to  
9 that described by Whale et al.<sup>42</sup> The apparatus employs a small (40 mm by 40 mm) aluminium cold  
10 stage thermally bonded to a TEC1-12704 Peltier thermoelectric cooler with Arctic Cooling MX-4  
11 thermal compound. A Meerstetter TEC-1091-PT100 Precision Peltier Controller drives the Peltier and  
12 allows for precise control of temperature of the coldstage. Temperature is monitored using two  
13 Netshushin PT100 platinum resistance thermometers (NR-141-100S-2-1.0-10-2000PLi-A-3) read by a  
14 PicoTech PT-104 data logger. The use of redundant PRTs allows detection of any significant  
15 temperature gradients or other issues in temperature measurement. The PRTs are embedded directly  
16 under the part of the cold stage used for ice nucleation measurements, meaning temperatures are  
17 recorded from a point as close to freezing droplets as possible. Quoted measurement uncertainty for the  
18 PT100s is  $\pm 0.15^\circ\text{C}$  although in practice both PRTs give the same reading to within a much smaller  
19 margin, typically  $0.05^\circ\text{C}$ . To prevent frost growth from interfering with experiments dry nitrogen gas  
20 is flowed over the droplets at a rate of 0.2 l/min. A video camera is used to monitor droplet freezing and  
21 custom LabView program used to link temperature measurements to video frames, allowing  
22 determination of freezing temperatures of individual droplets and therefore droplet fraction frozen and  
23 average freezing temperatures.

24 To conduct the experiments performed in this study arrays of 30 to 40 one  $\mu\text{l}$  droplets of the nucleator  
25 suspensions were pipetted onto a 22 mm diameter silanized slide (Hampton Research HR3-231) using  
26 a Sartorius Picus® electronic micropipette. One  $\mu\text{l}$  droplets of appropriate concentrations of salt  
27 solutions were then pipetted onto the nucleator-containing droplets to produce 2  $\mu\text{l}$  droplets containing  
28 known amounts of the nucleators and known concentrations of salts. The cold stage was then used to  
29 cool the droplets at a rate of  $2^\circ\text{C}$  per minute while droplet freezing was monitored as mentioned above.  
30 The error bars in Fig. 2 were calculated using a simple Monte-Carlo simulation based on that described  
31 by Vali.<sup>90</sup> A full description of the process is given in section S2 of the supplementary information.

32 The BCS376 feldspar sample used was the same powder used in the ice nucleation instrument  
33 intercomparison of DeMott et al.<sup>91</sup> and has a BET surface area of  $2.6\text{ m}^2\text{ g}^{-1}$ . The sample was originally  
34 obtained from the UK Bureau of Analysed samples and was ground to achieve the measured surface  
35 area. Figure S1 shows that the activity of this sample is similar to that of the BCS376 tested by Atkinson  
36 et al.<sup>15</sup> The *Betula pendula* pollen sample was purchased from Pharmallerga. The various salts were of  
37 reagent grade and purchased from Sigma Aldrich.

## 38 **Supplementary Material**

39 The online supplementary material contains discussion of the ice nucleation activity of the feldspar used  
40 in this study, details of the uncertainty analysis used, a discussion of the stabilities of ice Ih and ice XI,  
41 the literature fits used for the diffusion activation energy and ice-liquid interfacial tension, calculation  
42 of the heterogeneous ice nucleation rate of pollen washing water, discussion of the relationship between  
43 heterogeneous ice nucleation rate and the size of the ice critical cluster, calculations of the entropy  
44 change of spherical cap shaped ice clusters with addition of ammonium and calculation of the entropy  
45 change due to addition of ammonium ions to partially ordered ice cluster.

46

## 1 **Acknowledgment**

2 I gratefully acknowledge the Leverhulme Trust and the University of Warwick and for an Early Career  
3 Fellowship (ECF-127 2018) and Stephen Cox, Christoph Salzmann, Gabriele Sosso, Michael Whale  
4 and Martin Daily for helpful discussions.

## 5 **References**

- 6 <sup>1</sup>T. Bartels-Rausch, V. Bergeron, J. H. E. Cartwright, R. Escibano, J. L. Finney, H. Grothe, P. J.  
7 Gutiérrez, J. Haapala, W. F. Kuhs, J. B. C. Pettersson, S. D. Price, C. I. Sainz-Díaz, D. J. Stokes, G.  
8 Strazzulla, E. S. Thomson, H. Trinks, and N. Uras-Aytemiz, *Rev. Mod. Phys.* **84** (2012) 885.  
9 <sup>2</sup>C. G. Salzmann, *J. Chem. Phys.* **150** (2019) 060901.  
10 <sup>3</sup>T. Koop, and B. J. Murray, *J. Chem. Phys.* **145** (2016) 211915.  
11 <sup>4</sup>R. J. Herbert, B. J. Murray, S. J. Dobbie, and T. Koop, *Geophys. Res. Lett.* **42** (2015) 1599.  
12 <sup>5</sup>E. Sanz, C. Vega, J. R. Espinosa, R. Caballero-Bernal, J. L. F. Abascal, and C. Valeriani, *J. Am. Chem.*  
13 *Soc.* **135** (2013) 15008.  
14 <sup>6</sup>B. J. Murray, D. O'Sullivan, J. D. Atkinson, and M. E. Webb, *Chem. Soc. Rev.* **41** (2012) 6519.  
15 <sup>7</sup>Z. A. Kanji, L. A. Ladino, H. Wex, Y. Boose, M. Burkert-Kohn, D. J. Cziczo, and M. Krämer, *Meteorol.*  
16 *Monogr.* **58** (2017) 1.1.  
17 <sup>8</sup>T. Storelvmo, *Annu. Rev. Earth Planet. Sci.* **45** (2017) 199.  
18 <sup>9</sup>B. J. Murray, K. S. Carslaw, and P. R. Field, *Atmos. Chem. Phys.* **21** (2021) 665.  
19 <sup>10</sup>K. E. Zachariassen, and E. Kristiansen, *Cryobiology* **41** (2000) 257.  
20 <sup>11</sup>G. J. Morris, and E. Acton, *Cryobiology* **66** (2013) 85.  
21 <sup>12</sup>B. Vonnegut, *J. Appl. Phys.* **18** (1947) 593.  
22 <sup>13</sup>C. Marcolli, B. Nagare, A. Welti, and U. Lohmann, *Atmos. Chem. Phys.* **16** (2016) 8915.  
23 <sup>14</sup>L. R. Maki, E. L. Galyan, M.-M. Chang-Chien, and D. R. Caldwell, *Appl. Microbio.* **28** (1974) 456.  
24 <sup>15</sup>J. D. Atkinson, B. J. Murray, M. T. Woodhouse, T. F. Whale, K. J. Baustian, K. S. Carslaw, S. Dobbie,  
25 D. O'Sullivan, and T. L. Malkin, *Nature* **498** (2013) 355.  
26 <sup>16</sup>A. Kiselev, F. Bachmann, P. Pedevilla, S. J. Cox, A. Michaelides, D. Gerthsen, and T. Leisner, *Science*  
27 **355** (2017) 367.  
28 <sup>17</sup>G. C. Sosso, J. Chen, S. J. Cox, M. Fitzner, P. Pedevilla, A. Zen, and A. Michaelides, *Chem. Rev.* **116**  
29 (2016) 7078.  
30 <sup>18</sup>C. Blagden, *Philos. Trans. R. Soc.* **78** (1788) 277.  
31 <sup>19</sup>T. Koop, B. P. Luo, A. Tsias, and T. Peter, *Nature* **406** (2000) 611.  
32 <sup>20</sup>T. Koop, and B. Zobrist, *Phys. Chem. Chem. Phys.* **11** (2009) 10839.  
33 <sup>21</sup>B. Zobrist, C. Marcolli, T. Peter, and T. Koop, *J. Phys. Chem. A* **112** (2008) 3965.  
34 <sup>22</sup>A. Kumar, C. Marcolli, B. Luo, and T. Peter, *Atmos. Chem. Phys.* **18** (2018) 7057.  
35 <sup>23</sup>T. F. Whale, M. A. Holden, Theodore W. Wilson, D. O'Sullivan, and B. J. Murray, *Chem. Sci.* **9** (2018)  
36 4142.  
37 <sup>24</sup>Y. Boose, B. Sierau, M. I. García, S. Rodríguez, A. Alastuey, C. Linke, M. Schnaiter, P. Kupiszewski, Z.  
38 A. Kanji, and U. Lohmann, *Atmos. Chem. Phys.* **16** (2016) 9067.  
39 <sup>25</sup>A. Kumar, C. Marcolli, and T. Peter, *Atmos. Chem. Phys.* **19** (2019) 6059.  
40 <sup>26</sup>A. Kumar, C. Marcolli, and T. Peter, *Atmos. Chem. Phys.* **19** (2019) 6035.  
41 <sup>27</sup>R. J. Perkins, S. M. Gillette, T. C. J. Hill, and P. J. DeMott, *ACS Earth and Space Chem.* **4** (2020) 133.  
42 <sup>28</sup>J. Yun, N. Link, A. Kumar, A. Shchukarev, J. Davidson, A. Lam, C. Walters, Y. Xi, J.-F. Boily, and A. K.  
43 Bertram, *ACS Earth and Space Chem.* **4** (2020) 873.  
44 <sup>29</sup>M. T. Reischel, and G. Vali, *Tellus* **27** (1975) 414.  
45 <sup>30</sup>Y. Ren, A. K. Bertram, and G. N. Patey, *J. Phys. Chem. B* **124** (2020) 4605.  
46 <sup>31</sup>T. Inada, T. Koyama, F. Goto, and T. Seto, *J. Phys. Chem. B* **116** (2012) 5364.  
47 <sup>32</sup>T. Inada, T. Koyama, H. Tomita, T. Fuse, C. Kuwabara, K. Arakawa, and S. Fujikawa, *J. Phys. Chem. B*  
48 **121** (2017) 6580.

1 <sup>33</sup>S. Fujikawa, C. Kuwabara, J. Kasuga, and K. Arakawa, in *Survival Strategies in Extreme Cold and*  
2 *Desiccation: Adaptation Mechanisms and Their Applications*, edited by M. Iwaya-Inoue, M. Sakurai,  
3 and M. Uemura (Springer Singapore, Singapore, 2018), pp. 289.

4 <sup>34</sup>S. Curland, C. Allolio, L. Javitt, S. Dishon Ben-Ami, I. Weissbuch, D. Ehre, D. Harries, M. Lahav, and I.  
5 Lubomirsky, *Angew. Chem* **59** (2020) 15575.

6 <sup>35</sup>L. F. Javitt, I. Weissbuch, D. Ehre, I. Lubomirsky, and M. Lahav, *Cryst. Growth Des* **22** (2022) 43.

7 <sup>36</sup>S. E. Worthy, A. Kumar, Y. Xi, J. Yun, J. Chen, C. Xu, V. E. Irish, P. Amato, and A. K. Bertram, *Atmos.*  
8 *Chem. Phys.* **21** (2021) 14631.

9 <sup>37</sup>A. D. Harrison, T. F. Whale, M. A. Carpenter, M. A. Holden, L. Neve, D. O'Sullivan, J. Vergara  
10 Temprado, and B. J. Murray, *Atmos. Chem. Phys.* **16** (2016) 10927.

11 <sup>38</sup>A. D. Harrison, K. Lever, A. Sanchez-Marroquin, M. A. Holden, T. F. Whale, M. D. Tarn, J. B.  
12 McQuaid, and B. J. Murray, *Atmos. Chem. Phys.* **19** (2019) 11343.

13 <sup>39</sup>K. Dreischmeier, C. Budke, L. Wiehemeier, T. Kottke, and T. Koop, *Sci. Rep.* **7** (2017) 41890.

14 <sup>40</sup>B. G. Pummer, H. Bauer, J. Bernardi, S. Bleicher, and H. Grothe, *Atmos. Chem. Phys.* **12** (2012)  
15 2541.

16 <sup>41</sup>J. Fröhlich-Nowoisky, C. J. Kampf, B. Weber, J. A. Huffman, C. Pöhlker, M. O. Andreae, N. Lang-Yona,  
17 S. M. Burrows, S. S. Gunthe, W. Elbert, H. Su, P. Hoor, E. Thines, T. Hoffmann, V. R. Després and  
18 Ulrich Pöschl, *Atmos. Res.* **11** (2016) 346.

19 <sup>42</sup>T. F. Whale, B. J. Murray, D. O'Sullivan, T. W. Wilson, N. S. Umo, K. J. Baustian, J. D. Atkinson, D. A.  
20 Workneh, and G. J. Morris, *Atmos. Meas. Tech.* **8** (2015) 2437.

21 <sup>43</sup>A. Kumar, A. K. Bertram, and G. N. Patey, *ACS Earth and Space Chem.* **5** (2021) 2169.

22 <sup>44</sup>L. J. Conway, K. Brown, J. S. Loveday, and A. Hermann, *J. Chem. Phys.* **154** (2021) 204501.

23 <sup>45</sup>R. Brill, and S. Zaromb, *Nature* **173** (1954) 316.

24 <sup>46</sup>L. C. Labowitz, and E. F. Westrum, *J. Phys. Chem.* **65** (1961) 408.

25 <sup>47</sup>J. J. Shephard, B. Slater, P. Harvey, M. Hart, C. L. Bull, S. T. Bramwell, and C. G. Salzmänn, *Nature*  
26 *Physics* **14** (2018) 569.

27 <sup>48</sup>C. G. Salzmänn, Z. Sharif, C. L. Bull, S. T. Bramwell, A. Rosu-Finsen, and N. P. Funnell, *J. Phys. Chem.*  
28 *C* **123** (2019) 16486.

29 <sup>49</sup>Z. Sharif, J. J. Shephard, B. Slater, C. L. Bull, M. Hart, and C. G. Salzmänn, *J. Chem. Phys.* **154** (2021)  
30 114502.

31 <sup>50</sup>L. Pauling, *J. Am. Chem. Soc.* **57** (1935) 2680.

32 <sup>51</sup>Y. Tajima, T. Matsuo, and H. Suga, *Nature* **299** (1982) 810.

33 <sup>52</sup>J. D. Bernal, and R. H. Fowler, *J. Chem. Phys.* **1** (1933) 515.

34 <sup>53</sup>R. Feistel, and W. Wagner, *J. Phys. Chem. Ref. Data* **35** (2006) 1021.

35 <sup>54</sup>N. H. Fletcher, *J. Chem. Phys.* **30** (1959) 1476.

36 <sup>55</sup>T. Sayer, and S. J. Cox, *Phys. Chem. Chem. Phys.* **21** (2019) 14546.

37 <sup>56</sup>W. N. Lipscomb, *J. Chem. Phys.* **22** (1954) 344.

38 <sup>57</sup>C. P. Herrero, and R. Ramírez, *J. Chem. Phys.* **140** (2014) 234502.

39 <sup>58</sup>R. Cabriolu, and T. Li, *Phys. Rev. E* **91** (2015) 052402.

40 <sup>59</sup>B. Zobrist, T. Koop, B. P. Luo, C. Marcolli, and T. Peter, *J. Phys. Chem.* **111** (2007) 2149.

41 <sup>60</sup>G. D. Soria, J. R. Espinosa, J. Ramirez, C. Valeriani, C. Vega, and E. Sanz, *J. Chem. Phys.* **148** (2018)  
42 222811.

43 <sup>61</sup>T. L. Malkin, B. J. Murray, A. V. Brukhno, J. Anwar, and C. G. Salzmänn *Proc. Natl. Acad. Sci. U.S.A.*  
44 **109** (2012) 1041.

45 <sup>62</sup>T. L. Malkin, B. J. Murray, C. G. Salzmänn, V. Molinero, S. J. Pickering, and T. F. Whale, *Phys. Chem.*  
46 *Chem. Phys.* **17** (2015) 60.

47 <sup>63</sup>D. Quigley, *J. Chem. Phys.* **141** (2014) 121101.

48 <sup>64</sup>L. Lupi, A. Hudait, B. Peters, M. Grünwald, R. Gotchy Mullen, A. H. Nguyen, and V. Molinero,  
49 *Nature* **551** (2017) 218.

50 <sup>65</sup>M. B. Davies, M. Fitzner, and A. Michaelides, *Proc. Natl. Acad. Sci. U.S.A.* **118** (2021) e2025245118.

51 <sup>66</sup>D. Barahona, *Atmos. Chem. Phys.* **14** (2014) 7665.

1 <sup>67</sup> J. R. Espinosa, G. D. Soria, J. Ramirez, C. Valeriani, C. Vega, and E. Sanz, *J. Phys. Chem. Lett.* **8** (2017)  
2 4486.  
3 <sup>68</sup> D. M. Murphy, and T. Koop, *Q. J. R. Meteorol. Soc.* **131** (2005) 1539.  
4 <sup>69</sup> S. L. Clegg, P. Brimblecombe, and A. S. Wexler, *J. Phys. Chem. A* **102** (1998) 2155.  
5 <sup>70</sup> M. A. Holden, T. F. Whale, M. D. Tarn, D. O'Sullivan, R. D. Walshaw, B. J. Murray, F. C. Meldrum,  
6 and H. K. Christenson, *Sci. Adv.* **5** (2019) eaav4316.  
7 <sup>71</sup> R. J. Herbert, B. J. Murray, T. F. Whale, S. J. Dobbie, and J. D. Atkinson, *Atmos. Chem. Phys.* **14**  
8 (2014) 8501.  
9 <sup>72</sup> D. Barahona, *Atmos. Chem. Phys.* **18** (2018) 17119.  
10 <sup>73</sup> G. W. Gross, P. M. Wong, and K. Humes, *J. Chem. Phys.* **67** (1977) 5264.  
11 <sup>74</sup> O. M. Magnussen, and A. Groß, *J. Am. Chem. Soc.* **141** (2019) 4777.  
12 <sup>75</sup> T. Sayer, and S. J. Cox, *J. Chem. Phys.* **153** (2020) 164709.  
13 <sup>76</sup> G. C. Sosso, G. A. Tribello, A. Zen, P. Pedevilla, and A. Michaelides, *J. Chem. Phys.* **145** (2016)  
14 211927.  
15 <sup>77</sup> X. L. Hu, and A. Michaelides, *Surf. Sci.* **604** (2010) 111.  
16 <sup>78</sup> Y. Gan, and G. V. Franks, *Langmuir* **22** (2006) 6087.  
17 <sup>79</sup> A. Kiselev, A. Keinert, T. Gaedecke, T. Leisner, C. Sutter, E. Petrishcheva, and R. Abart, *Atmos.*  
18 *Chem. Phys.* **21** (2021) 11801.  
19 <sup>80</sup> J. Goniakowski, F. Finocchi, and C. Noguera, *Rep. Prog. Phys.* **71** (2007) 016501.  
20 <sup>81</sup> G. Vali, *Atmos. Chem. Phys.* **14** (2014) 5271.  
21 <sup>82</sup> T. F. Whale, M. A. Holden, A. N. Kulak, Y.-Y. Kim, F. C. Meldrum, H. K. Christenson, and B. J. Murray,  
22 *Phys. Chem. Chem. Phys.* **19** (2017) 31186.  
23 <sup>83</sup> A. A. Kiselev, A. Keinert, T. Gaedecke, T. Leisner, C. Sutter, E. Petrishcheva, and R. Abart, *Atmos.*  
24 *Chem. Phys.* **21** (2021) 11801.  
25 <sup>84</sup> N. N. Lata, J. Zhou, P. Hamilton, M. Larsen, S. Sarupria, and W. Cantrell, *J. Phys. Chem. Lett.* **11**  
26 (2020) 8682.  
27 <sup>85</sup> S. Jin, Y. Liu, M. Deiseroth, J. Liu, E. H. G. Backus, H. Li, H. Xue, L. Zhao, X. C. Zeng, M. Bonn, and J.  
28 Wang, *J. Am. Chem. Soc.* **142** (2020) 17956.  
29 <sup>86</sup> A. Abdelmonem, E. H. G. Backus, N. Hoffmann, M. A. Sánchez, J. D. Cyran, A. Kiselev, and M. Bonn,  
30 *Atmos. Chem. Phys.* **17** (2017) 7827.  
31 <sup>87</sup> S. Curland, L. Javitt, I. Weissbuch, D. Ehre, M. Lahav, and I. Lubomirsky, *Angew. Chem* **59** (2020)  
32 15570.  
33 <sup>88</sup> M. Shrivastava, C. D. Cappa, J. Fan, A. H. Goldstein, A. B. Guenther, J. L. Jimenez, C. Kuang, A.  
34 Laskin, S. T. Martin, N. L. Ng, T. Petaja, J. R. Pierce, P. J. Rasch, P. Roldin, J. H. Seinfeld, J. Shilling, J. N.  
35 Smith, J. A. Thornton, R. Volkamer, J. Wang, D. R. Worsnop, R. A. Zaveri, A. Zelenyuk, and Q. Zhang,  
36 *Rev. Geophys.* **55** (2017) 509.  
37 <sup>89</sup> M. Ehn, J. A. Thornton, E. Kleist, M. Sipilä, H. Junninen, I. Pullinen, M. Springer, F. Rubach, R.  
38 Tillmann, B. Lee, F. Lopez-Hilfiker, S. Andres, I.-H. Acir, M. Rissanen, T. Jokinen, S. Schobesberger, J.  
39 Kangasluoma, J. Kontkanen, T. Nieminen, T. Kurtén, L. B. Nielsen, S. Jørgensen, H. G. Kjaergaard, M.  
40 Canagaratna, M. D. Maso, T. Berndt, T. Petäjä, A. Wahner, V.-M. Kerminen, M. Kulmala, D. R.  
41 Worsnop, J. Wildt, and T. F. Mentel, *Nature* **506** (2014) 476.  
42 <sup>90</sup> G. Vali, *Atmos. Meas. Tech.* **12** (2019) 1219.  
43 <sup>91</sup> P. J. DeMott, O. Möhler, D. J. Cziczo, N. Hiranuma, M. D. Petters, S. S. Petters, F. Belosi, H. G.  
44 Bingemer, S. D. Brooks, C. Budke, M. Burkert-Kohn, K. N. Collier, A. Danielczok, O. Eppers, L.  
45 Felgitsch, S. Garimella, H. Grothe, P. Herenz, T. C. J. Hill, K. Höhler, Z. A. Kanji, A. Kiselev, T. Koop, T.  
46 B. Kristensen, K. Krüger, G. Kulkarni, E. J. T. Levin, B. J. Murray, A. Nicosia, D. O'Sullivan, A. Peckhaus,  
47 M. J. Polen, H. C. Price, N. Reicher, D. A. Rothenberg, Y. Rudich, G. Santachiara, T. Schiebel, J. Schrod,  
48 T. M. Seifried, F. Stratmann, R. C. Sullivan, K. J. Suski, M. Szakáll, H. P. Taylor, R. Ullrich, J. Vergara-  
49 Temprado, R. Wagner, T. F. Whale, D. Weber, A. Welti, T. W. Wilson, M. J. Wolf, and J. Zenker,  
50 *Atmos. Meas. Tech.* **11** (2018) 6231.